Contribution of high risk groups' unmet needs may be underestimated in epidemic models without risk turnover: a mechanistic modelling analysis ☆

Jesse Knight[a], Stefan D. Baral[b], Sheree Schwartz[b], Linwei Wang[a], Huiting Ma[a], Katherine Young[c], Harry Hausler[c], Sharmistha Mishra[a,d,e,f,*]

[a]MAP Centre for Urban Health Solutions, Unity Health Toronto
[b]Deptartment of Epidemiology, Johns Hopkins Bloomberg School of Public Health
[c]TB HIV Care, South Africa
[d]Department of Medicine, Division of Infectious Disease, University of Toronto
[e]Institute of Health Policy, Management and Evaluation, Dalla Lana School of Public Health, University of Toronto
[f]Instituof Medical Sciences, University of Toronto

Abstract

BACKGROUND. Epidemic models of sexually transmitted infections (STIs) are often used to characterize the contribution of risk groups to overall transmission by projecting the transmission population attributable fraction (tPAF) of unmet prevention and treatment needs within risk groups. However, evidence suggests that STI risk is dynamic over an individual's sexual life course, which manifests as turnover between risk groups. We sought to examine the mechanisms by which turnover influences modelled projections of the tPAF of high risk groups. METHODS. We developed a unifying, data-guided framework to simulate risk group turnover in deterministic, compartmental transmission models. We applied the framework to an illustrative model of an STI and examined the mechanisms by which risk group turnover influenced equilibrium prevalence across risk groups. We then fit a model with and without turnover to the same risk-stratified STI prevalence targets and compared the inferred level of risk heterogeneity and tPAF of the highest risk group projected by the two models. RESULTS. The influence of turnover on group-specific prevalence was mediated by three main phenomena: movement of previously high risk individuals with the infection into lower risk groups; changes to herd immunity in the highest risk group; and changes in the number of partnerships where transmission can occur. Faster turnover led to a smaller ratio of STI prevalence between the highest and lowest risk groups. Compared to the fitted model without turnover, the fitted model with turnover inferred greater risk heterogeneity and consistently projected a larger tPAF of the highest risk group over time. IMPLICATIONS. If turnover is not captured in epidemic models, the projected contribution of high risk groups, and thus, the potential impact of prioritizing interventions to address their needs, could be underestimated. To aid the next generation of tPAF models, data collection efforts to parameterize risk group turnover should be prioritized.

Highlights

1. A new framework for parameterizing turnover in risk groups is developed

2. Mechanisms by which turnover influences STI prevalence in risk groups are examined

3. Turnover reduces the ratio of equilibrium STI prevalence in high vs low risk groups

4. Inferred risk heterogeneity is higher when fitting transmission models with turnover

5. Ignoring turnover in risk could underestimate the tPAF of high risk groups

Keywords: mathematical modelling, transmission, risk heterogeneity, turnover, sexually transmitted infection, population attributable fraction

---

☆ On behalf of the Siyaphambili study team

∗ Corresponding author (`sharmistha.mishra@utoronto.ca`)

Abbreviations: STI: sexually transmitted infection, HIV: human immunodeficiency virus, tPAF: transmission population attributable fraction

Contents

1. Introduction

Heterogeneity in transmission risk is a consistent characteristic of epidemics of sexually transmitted infections (STI) (Anderson and May, 1991). This heterogeneity is often demarcated by identifying specific populations whose risks of acquisition and onward transmission of STI are the highest, such that their specific unmet prevention and treatment needs can sustain local epidemics of STI (Yorke et al., 1978). Disproportionate risk can be conferred in several ways at the individual-level (higher number of sexual partners), partnership-level (reduced condom use within specific partnership types), or structural-level (stigma as a barrier to accessing prevention and treatment services) (Baral et al., 2013). The contribution of high risk groups to the overall epidemic can then be used as an indicator in the appraisal of STI epidemics, helping to guide intervention priorities (Shubber et al., 2014; Mishra et al., 2016).

Traditionally, contribution to an epidemic was quantified using either: the classic *population attributable fraction* (PAF) via the relative risk of incident infections within a risk group versus the rest of the population and the relative size of the risk group (Hanley, 2001); or the distribution of new infections across subsets of a population (Case et al., 2012; Mishra et al., 2014). So when small risk groups experience disproportionately higher rate of incident infections – e.g. 5 percent of a population acquire 30 percent of STI infections – contribution is interpreted as 5 percent of the population contributing to 30 percent of all infections (Prüss-Ustün et al., 2013). However, the classic PAF does not account for chains of (indirect) transmission, and has been shown to underestimate the contribution of some higher-risk groups to cumulative STI infections, especially over time (Mishra et al., 2014). Thus, transmission models are increasingly being used to quantify contribution by accounting for indirect transmission and projecting the *transmission population attributable fraction* (tPAF). The tPAF is calculated by simulating counterfactual scenarios where transmission between specific subgroups is stopped, and the relative difference in cumulative infections in the total population over various time-periods is measured (Mishra et al., 2014; Mukandavire et al., 2018). Transmission can be stopped by setting susceptibility and/or infectiousness to zero in the model (Mishra et al., 2014). The tPAF is then interpreted as the fraction of all new infections that stem, directly and indirectly, from a failure to prevent acquisition and/or to provide effective treatment in a particular risk group (Mishra et al., 2016; Mukandavire et al., 2018; Maheu-Giroux et al., 2017).

There is limited evidence on how model structure might influence the tPAF of higher risk groups (Mishra et al., 2016; Mukandavire et al., 2018; Maheu-Giroux et al., 2017), especially movement of individuals between risk groups, an epidemiologic phenomenon that is well-described in the context of sexual behaviour (Watts et al., 2010). Such movement is often referred to in the STI epidemiology literature as *turnover* (Watts et al., 2010). For example, turnover may reflect entry into or retirement from formal sex work, or other periods associated with higher STI susceptibility and onward transmission due to more partners and/or vulnerabilities (Marston and King, 2006; Watts et al., 2010). Risk group turnover has been shown

1

to influence the predicted equilibrium prevalence of an STI (Stigum et al., 1994; Zhang et al., 2012); the fraction of transmissions occurring during acute HIV infection (Zhang et al., 2012); the basic reproductive number R_0 (Henry and Koopman, 2015); and the coverage of antiretroviral therapy required to achieve HIV epidemic control (Henry and Koopman, 2015). Yet how, and the extent to which, turnover influences tPAF has yet to be examined.

There is variability in how turnover has been previously implemented (Stigum et al., 1994; Koopman et al., 1997; Eaton and Hallett, 2014; Boily et al., 2015), in large part because of four main assumptions or epidemiologic constraints surrounding movement between risk groups. For example, in the context of turnover, the relative size of specific populations in the model may be constrained to remain constant over time (Stigum et al., 1994; Koopman et al., 1997; Eaton and Hallett, 2014), such as the proportion of individuals who sell sex. Second, some individuals may enter into high risk groups at an early age, and subsequently settle into lower risk groups; thus the distribution of risks among individuals entering into the transmission model may be assumed to be different from the distribution of risks among individuals already in the transmission model (Eaton and Hallett, 2014). Third, turnover may be constrained to reflect the average duration of time spent within a given risk group (Boily et al., 2015), such as duration engaged in formal sex work (Watts et al., 2010). Finally, turnover could reflect data on how sexual behaviour changes following exit from a given risk group (Boily et al., 2015). Most prior models used some combination of these constraints, based on their specific data or research question, but to date there is no unified approach to modelling turnover.

In this study, we explored the mechanisms by which turnover may influence the tPAF of a high risk group using an illustrative STI model with treatment-induced immunity and without STI-attributable mortality. First, we developed a unified approach to implementing turnover based on epidemiologic constraints. We then sought the following objectives: 1) understand the mechanisms by which turnover influences group-specific STI prevalence and ratios of prevalence between risk groups; 2) examine how inclusion/exclusion of turnover in a model influences the level of risk heterogeneity inferred during model fitting; and 3) examine how inclusion/exclusion of turnover in a model influences the projected tPAF of the highest risk group after model fitting to a particular setting.

2. Methods

We developed a new, unified framework for implementing turnover. We then simulated a deterministic compartmental model of an illustrative STI, with turnover as per the framework, to conduct out experiments.

2.1. A unified framework for implementing turnover

We developed a framework for implementing turnover, as depicted in Figure 1 and detailed in Appendix A. In the framework, the simulated population is divided into G risk groups. The number of
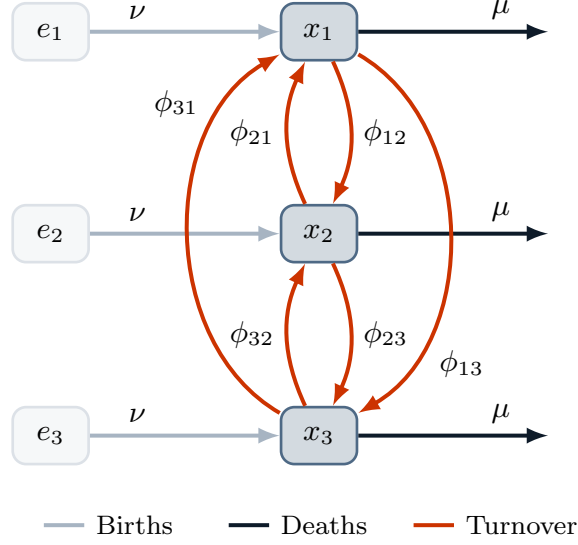
Figure 1: System of $G = 3$ risk groups and turnover between them.

x_i: number of individuals in risk group i; e_i: number of individuals available to enter risk group i; ν: rate of population entry; μ: rate of population exit; ϕ_{ij}: rate of turnover from group i to group j.

individuals in group $i \in [1, \ldots, G]$ is denoted x_i, and the relative size of each group is denoted $\hat{x}_i = x_i/N$, where N is the total population size. Individuals enter the population at a rate ν and exit at a rate μ per year. The distribution of risk groups at entry into the model is denoted $\hat{e}_i$, which may be different from $\hat{x}_i$. The total number of individuals entering group i per year is therefore given by $\nu \hat{e}_i N$. Turnover rates are collected in a $G \times G$ matrix ϕ, where ϕ_{ij} is the proportion of individuals in group i who move from group i into group j each year. The framework is independent of the disease model, and thus transition rates ϕ do not depend on health states.

The framework assumes that: 1) the relative sizes of risk groups $\hat{\boldsymbol{x}} = [\hat{x}_1, \ldots, \hat{x}_G]$ are known and should remain constant over time; and 2) the rates of population entry ν and exit μ are known, but that they may vary over time. An approach to estimate ν and μ is detailed in Appendix A.2.1. The framework then provides a method to estimate the values of the parameters $\hat{\boldsymbol{e}}$ and ϕ, representing G and $G(G - 1) = G^2$ total unknowns. In the framework, $\hat{\boldsymbol{e}}$ and ϕ are collected in the vector $\boldsymbol{\theta} = [\hat{\boldsymbol{e}}, \boldsymbol{y}]$, where $\boldsymbol{y} = \text{vec}_{i \neq j}(\phi)$. To uniquely determine the elements of $\boldsymbol{\theta}$, a set of linear constraints are constructed. Each constraint k takes the form $b_k = A_k \boldsymbol{\theta}$, where b_k is a constant and A_k is a vector with the same length as $\boldsymbol{\theta}$. The values of $\boldsymbol{\theta}$ are then obtained by solving:

$$\boldsymbol{b} = A \boldsymbol{\theta} \tag{1}$$

using existing algorithms for solving linear systems (LAPACK, 1992).

The framework defines four types of constraints, which are based on assumptions, that can used to solve for the values of $\hat{\boldsymbol{e}}$ and ϕ via $\boldsymbol{\theta}$. The frameworks is flexible with respect to selecting and combining these

Table 1: Summary of constraint types for defining risk group turnover

Constraint	Assumption	Parameters	Types of data sources for parameterization
1. Constant group size	the relative population sizes of groups are known or assumed, and assumed to not change over time	$\hat{x}_i$	demographic health surveys (The DHS Program, 2019), key population mapping and enumeration (Abdul-Quader et al., 2014)
2. Specified elements	the relative numbers of people entering into each group upon entry into the model or after leaving another group are known or assumed	$\hat{e}_i, \phi_{ij}$	demographic health surveys (The DHS Program, 2019), key population surveys (Baral et al., 2014)
3. Group duration	the average durations of individuals in each group are known or assumed	δ_i	cohort studies of sexual behaviour over time (Fergus et al., 2007), key population surveys (Watts et al., 2010; Baral et al., 2014)
4. Turnover rate ratios	ratios between different rates of turnover are known or assumed	ϕ_{ij}	demographic health surveys (The DHS Program, 2019), key population surveys (Baral et al., 2014)

ϕ_{ij}: rate of turnover from group i to group j; $\hat{x}_i$: proportion of individuals in risk group i; $\hat{e}_i$: proportion of individuals entering into risk group i; δ_i: average duration spent in risk group i.
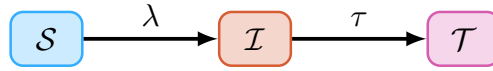

Figure 2: Modelled health states: $\mathcal{S}$: susceptible; $\mathcal{I}$: infected; $\mathcal{T}$: treated; and transitions: λ: force of infection; τ: treatment.

constraints, guided by the availability of data. However, exactly G^2 non-redundant constraints must be specified to produce a unique solution, such that exactly one value of $\boldsymbol{\theta}$ satisfies all constraints. Table 1 summarizes the four types of constraints, with their underlying assumptions, and the types of data that can be used in each case. Additional details, including constraint equations, examples, and considerations for combining constraints, are in Appendix A.2.2.

2.2. Transmission model

We developed a deterministic, compartmental model of an illustrative sexually transmitted infection with 3 risk groups. We did not simulate a specific pathogen, but rather constructed a biological system that included susceptible, infectious, and treated (or recovered/immune) health states. The transmission model therefore was mechanistically representative of sexually transmitted infections like HIV, where effective antiretroviral treatment represents a health state where individuals are no longer susceptible nor infectious (Maartens et al., 2014), or hepatitis B virus, where a large proportion of individuals who clear their acute infection develop life-long protective immunity (Ganem and Prince, 2004).

The model is represented by a set of coupled ordinary differential equations (Appendix B.1) and includes three health states: susceptible $\mathcal{S}$, infectious $\mathcal{I}$, and treated $\mathcal{T}$ (Figure 2), and $G = 3$ levels of risk: high H, medium M, and low L. Risk strata are defined by different number of partners per year, so that individuals

4

in risk group i are assumed to form partnerships at a rate C_i per year. The probability of partnership formation ρ_{ik} between individuals in group i and individuals in risk group k is assumed to be proportionate to the total number of available partnerships within each group Garnett and Anderson (1994):

$$\rho_{ik} = \frac{C_k x_k}{\sum_{\mathrm{k}} C_{\mathrm{k}} x_{\mathrm{k}}} \tag{2}$$

The biological probability of transmission is defined as β per partnership. Individuals transition from the susceptible $\mathcal{S}$ to infectious $\mathcal{I}$ health state via a force of infection λ_i per year, per susceptible in risk group i:

$$\lambda_i = C_i \sum_k \rho_{ik} \, \beta \, \frac{\mathcal{I}_k}{x_k} \tag{3}$$

Individuals are assumed to transition from the infectious $\mathcal{I}$ to treated $\mathcal{T}$ health state at a rate τ per year, reflecting diagnosis and treatment. The treatment rate does not vary by risk group. Individuals in the treated $\mathcal{T}$ health state are neither infectious nor susceptible, and individuals cannot become re-infected.

2.2.1. Implementing turnover within the transmission model

As described in Section 2.1, individuals enter the model at a rate ν, exit the model at a rate μ, and transition from risk group i to group j at a rate ϕ_{ij}, health state. The turnover rates ϕ and distribution of individuals entering the model by risk group $\hat{e}$ were computed using the methods outlined in Appendix A.2.2, based on the following three assumptions. First, we assumed that the proportion of individuals entering each risk group $\hat{e}$ was equal to the proportion of individuals across risk groups in the model $\hat{x}$. Second, we assumed that the average duration of time spent in each risk group δ was known. Third, we assumed that the absolute number of individuals moving between two risk groups in either direction was balanced, meaning that if 10 individuals moved from group i to group j, then another 10 individuals moved from group j to group i. These three assumptions were selected because they reflect the common assumptions underlying turnover in prior models (Zhang et al., 2012; Henry and Koopman, 2015) and also to avoid any dominant direction of turnover. That is, we wanted to study the influence of movement between risk groups in general, as compared to no movement, and at various rates of movement, rather than movement predominantly from some groups to some other groups. The system of equations formulated from the above assumptions and constraints is given in Appendix B.2. To satisfy all three assumptions, there was only one possible value for each element in ϕ and $\hat{e}$. That is, by specifying these three assumptions, we generated a unique set of ϕ and $\hat{e}$.

Under the above three assumptions, we still needed to specify the particular values of the parameters $\hat{x}$, δ, ν, and μ. Such parameter values could be derived from data as described in Appendix A.2.2. However, in all our experiments, we used the illustrative values summarized in Table 2. After resolving the system of

Table 2: Default model parameters for experiments

Symbol	Description	Default value
β	transmission probability per partnership	0.03
τ	rate of treatment initiation among infected	0.1
N_0	initial population size	1000
$\hat{\boldsymbol{x}}$	proportion of system individuals by risk group	[0.05 0.20 0.75]
$\hat{\boldsymbol{e}}$	proportion of entering individuals risk by risk group	[0.05 0.20 0.75]
$\boldsymbol{\delta}$	average duration spent in each risk group	[5 15 25]
C	number of partners per year by individuals in each risk group	[25 5 1]
ν	rate of population entry	0.05
μ	rate of population exit	0.03

All rates have units year^{-1}; durations are in years; parameters stratified by risk group are written [high, medium, low] risk.

equations Eq. (1) using these values, $\hat{\boldsymbol{e}}$ was equal to $\hat{\boldsymbol{x}}$ (assumed), and ϕ was:

$$\phi = \begin{bmatrix} * & 0.0833 & 0.0867 \\ 0.0208 & * & 0.0158 \\ 0.0058 & 0.0042 & * \end{bmatrix} \tag{4}$$

We then simulated epidemics using ϕ above and the parameters shown in Table 2. The transmission model was initialized with $N_0 = 1000$ individuals who were distributed across risk groups according to $\hat{\boldsymbol{x}}$. We seeded the epidemic with one infectious individual in each risk group at $t = 0$ in an otherwise fully susceptible populatuon. We numerically solved the system of ordinary differential equations (Appendix B.1) in Python using Euler's method with a time step of $dt = 0.1$ years. Code for all aspects of the project is available at: https://github.com/c-uhs/turnover.

2.3. Experiments

We designed three experiments to examine the influence of turnover on simulated epidemics. We analyzed all outcomes at equilibrium, defined as steady state at $t = 500$ years with $< 1\%$ change in incidence per year.

2.3.1. Experiment 1: Mechanisms by which turnover influences equilibrium prevalence

We designed Experiment 1 to explore the mechanisms by which turnover influences the equilibrium STI prevalence of infection, and the ratio of prevalence between risk groups (prevalence ratios). We defined prevalence as $\hat{\mathcal{I}}_i = \dfrac{\mathcal{I}_i}{x_i}$. Similar to previous studies (Zhang et al., 2012; Henry and Koopman, 2015), we varied the rates of turnover using a single parameter. However, because our model had $G = 3$ risk groups, multiplying a set of base rates ϕ by a scalar factor would change the relative population sizes of risk groups $\hat{\boldsymbol{x}}$.
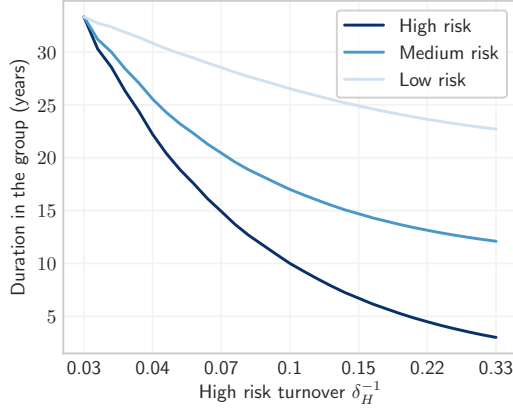
Figure 3: Average duration of time spent in each risk group versus turnover.

Turnover rate (log scale) is a function of the duration of time spent in the high risk group δ_H, where shorter time spent in the high risk group yields faster turnover. No turnover is indicated by $\delta_H^{-1} = 0.03$, due to population exit rate $\mu = 0.03$.

Instead of a scalar factor, we controlled the rates of turnover using the duration of time spent in the high risk group δ_H, because of the practical interpretation of δ_H in the context of STI transmission, such as the duration in formal sex work (Watts et al., 2010). A shorter δ_H yielded faster rates of turnover among all groups. The duration of time spent in the medium risk group δ_M was then defined as a value between δ_H and the maximum duration μ^{-1} which scaled with δ_H following: $\delta_M = \delta_H + \kappa \left(\mu^{-1} - \delta_H \right)$, with $\kappa = 0.3$. The duration of time in the low risk group δ_L similarly scaled with δ_H, but due to existing constraints, specification of δ_H and δ_M ensured only one possible value of δ_L. Thus, each value of δ_H yielded a unique set of turnover rates ϕ whose elements all scaled inversely with the duration in the high risk group δ_H.

We varied δ_H across a range of 33 to 3 years, reflecting a range from the full duration of simulated sexual activity $\mu^{-1} \approx 33$ years, through an average reported duration in sex work as low as 3 years (Watts et al., 2010). The resulting duration of time spent in each group versus turnover in the high risk group δ_H^{-1} is shown in Figure 3. For each set of turnover rates, we plotted the equilibrium prevalence in each risk group, and the prevalence ratios between high/low, high/medium, and medium/low risk groups. In order to understand the mechanisms by which turnover influenced prevalence and prevalence ratios (Objective 1), we additionally plotted the four components which contributed to gain/loss of infectious individuals in each risk group, based on Eq. (B.1b): 1) net gain/loss via turnover of infectious individuals, 2) gain via incident infections, 3) loss via treatment, and 4) loss via death. The influence of turnover on prevalence was only mediated by components 1 and 2, since components 3 and 4 were defined as constant rates which did not change with turnover; as such, our analysis focused on components 1 and 2. Finally, to further understand trends in incident infections versus turnover (component 1), we factored equation Eq. (3) for incidence λ_i into constant and non-constant factors, and plotted the non-constant factors versus turnover.

2.3.2. Experiment 2: Inferred risk heterogeneity with vs without turnover

We designed Experiment 2 to examine how the inclusion versus exclusion of turnover influences the inference of transmission model parameters related to risk heterogeneity, specifically the numbers of partners per year C_i across risk groups. The ratio of partner numbers C_H / C_L is one way to measure of how different the two risk groups are with respect to acquisition and transmission risks. Indeed, ratios of partner numbers are often used when parameterizing risk heterogeneity in STI transmission models (Mishra et al., 2012).

First, we fit the transmission model with turnover and without turnover, to equilibrium infection prevalence across risk groups. Specifically, we held all other parameters at their default values and fit the numbers of partners per year in each risk group C_i to reproduce the following: 20% infection prevalence among the high risk group, 8.75% among the medium risk group, 3% among the low risk group, and 5% overall. To identify the set of parameters (i.e. partner numbers C in each risk group) that best reproduced the fitting targets, we minimized the negative log-likelihood of group-specific and overall prevalence. Sample sizes of 500, 2000, 7500, and 10,000 were assumed to generate binomial distributions for the high, medium, low, and overall prevalence targets respectively, reflecting typical sample sizes in nationally representative demographic and health surveys (The DHS Program, 2019), multiplied by the relative sizes of risk groups in the model $\hat{\boldsymbol{x}}$. The minimization was performed using the SLSQP method (Kraft, 1988) from the SciPy Python `minimize` package. To address Objective 2, we compared the fitted (posterior) ratio of partners per year C_H / C_L in the model with turnover versus the model without turnover.

2.3.3. Experiment 3: Influence of turnover on the tPAF of the high risk group

We designed Experiment 3 to examine how the tPAF of the high risk group varies when projected by a model with versus without turnover (Objective 3). We calculated the tPAF of risk group i by comparing the relative difference in cumulative incidence between a base scenario, and a counterfactual where transmission from group i is turned off, starting at the fitted equilibrium. That is, in the counterfactual scenario, infected individuals in the high risk group could not transmit the infection. The tPAF was calculated over different time-horizons (1 to 50 years) as (Mishra et al., 2014):

$$\text{tPAF}_i(t) = \frac{\displaystyle\int_{t_{eq}}^{t} I_b(\tau)\,d\tau - \int_{t_{eq}}^{t} I_c(\tau)\,d\tau}{\displaystyle\int_{t_{eq}}^{t} I_b(\tau)\,d\tau} \tag{5}$$

where t_{eq} is the time corresponding to equilibrium, $I_b(t)$ is the rate of new infections at time t in the base scenario, and $I_c(t)$ is the rate of new infections at time t in the counterfactual scenario. We then compared the tPAF generated from the fitted model with turnover to the tPAF generated from the fitted model without turnover.
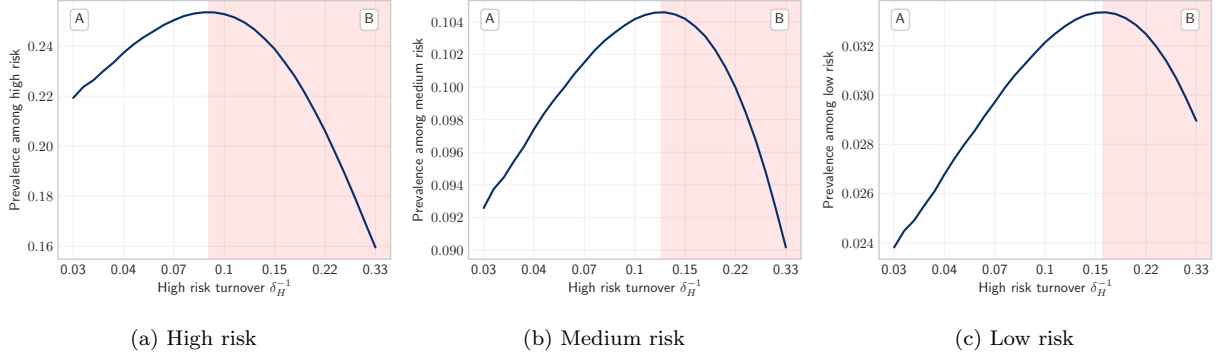
8

| (a) High risk | (b) Medium risk | (c) Low risk |

Figure 4: Relationship between equilibrium STI prevalence in high, medium, and low risk groups versus turnover rate. Regions A and B denote where equilibrium prevalence is increasing and decreasing with different rates of turnover, respectively. Turnover rate (log scale) is a function of the duration of time spent in the high risk group δ_H, where shorter time spent in the high risk group yields faster turnover. No turnover is indicated by $\delta_H^{-1} = 0.03$, due to population exit rate $\mu = 0.03$.

3. Results

3.1. Experiment 1: Mechanisms by which turnover influences equilibrium prevalence

Figure 4 shows the trends in equilibrium STI prevalence among the high (a), medium (b), and low (c) risk groups, at different rates of turnover which are depicted on the x-axis, based on duration of time spent in the high risk group. Figure 4 reveals an inverted U-shaped relationship between STI prevalence and turnover in all three risk groups. That is, equilibrium STI prevalence was higher in systems with slow turnover versus those with no turnover (Figure 4, region A). Equilibrium STI prevalence then peaked at slightly faster turnover before declining in systems with even faster turnover (region B in Figure 4). Comparison of group-specific prevalence in Figure 4 shows that the threshold turnover rate at which group-specific prevalence peaked varied by risk group: prevalence in the high risk group peaked at the lower turnover threshold (Figure 4a), while prevalence in low risk group peaked at a higher turnover threshold (Figure 4c). To explain the inverted U-shape and different turnover thresholds by group, we examined the components contributing to prevalence, first in the high risk group, and then in the low risk group.

Figure 5 shows the yearly gain/loss of individuals via turnover, and gain/loss via incident infections, in each health state and risk group, at equilibrium under different rates of turnover. Figure 6 also illustrates the distribution of health states in each risk group and among individuals moving between risk groups under four different rates of turnover.

3.1.1. Influence of turnover on equilibrium prevalence in the high risk group

As shown in Figure 6, at all four rates of turnover the proportion of individuals who were in the infectious state (STI prevalence) was largest in the high risk group. As infectious individuals left the high risk group via turnover, they were largely replaced by susceptible individuals from lower risk groups (Figure 6b and

(a) High risk susceptible   (b) High risk infectious   (c) High risk treated

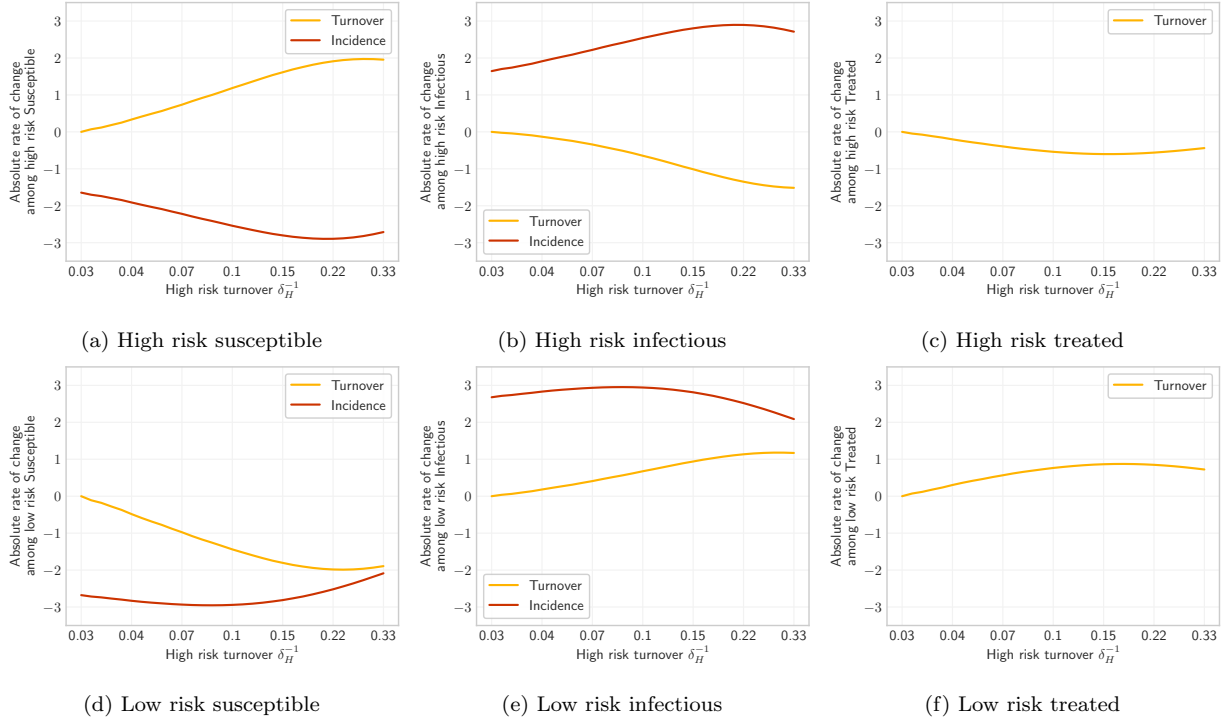(d) Low risk susceptible   (e) Low risk infectious   (f) Low risk treated

Figure 5: Absolute rates of change at equilibrium (number of individuals gained/lost per year) among individuals in each health state and risk group, due to: loss/gain via turnover (yellow), and loss/gain via incident infections (red). Based on Eq. (B.1). See Figure C.2 for all derivative components.

Turnover rate (log scale) is a function of the duration of time spent in the high risk group δ_H, where shorter time spent in the high risk group yields faster turnover. No turnover is indicated by $\delta_H^{-1} = 0.03$, due to population exit rate $\mu = 0.03$.

Figures 5a vs 5b, yellow). The pattern of net outflow of infectious individuals from the high risk group via turnover persisted across the range of turnover rates (Figure 5b, yellow). This net outflow of infectious individuals via turnover acted to reduce STI prevalence in the high risk group (phenomenon 1). Treated individuals were similarly replaced largely by susceptible individuals (Figure 6b and Figures 5a vs 5c, yellow). The net replacement of both infectious and treated individuals with susceptible individuals in the high risk group acted to reduce herd immunity in that group. Reduced herd immunity then contributed to a rise in the number of incident infections in the high risk group, as the system moved from no turnover to slow turnover (Figure 5b, red; phenomenon 2). Incidence was further influenced by a third phenomenon as systems moved from no turnover to higher rates of turnover: the net movement of infectious individuals from high to low risk (Figure 6b) reduced the average number of partners per year made available by individuals in the infectious state (Figure 7a). As shown in Appendix B.4, modelled incidence in all risk groups was proportional to the average number of partners per year among infectious individuals (Figure 7a), and overall prevalence (Figure 7b). Thus, as the average number of partners per year among infectious individuals fell with faster turnover, incidence decreased (Figure 7c, region B; phenomenon 3).
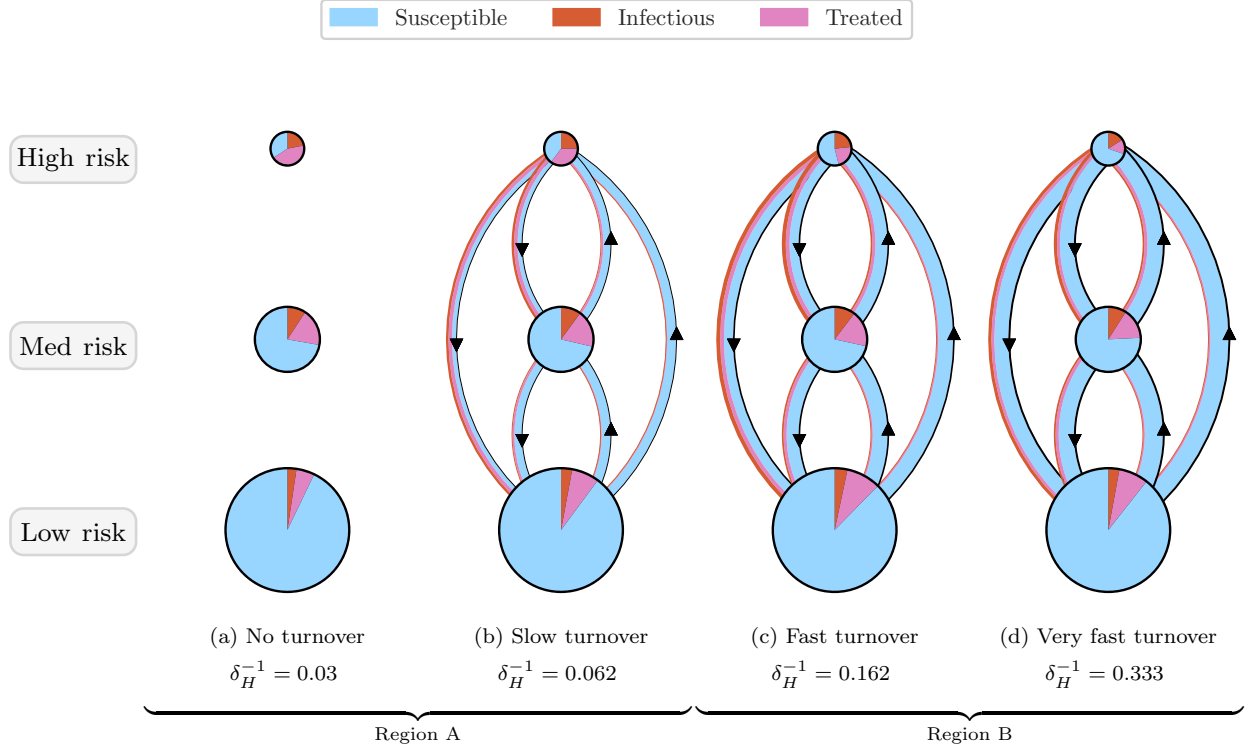
10

Figure 6: Depiction of health states of individuals in each risk group and of individuals moving between risk groups, obtained from models at equilibrium under four overall rates of turnover.

Circle sizes are proportional to risk group sizes. Circle slices and arrow widths are also proportional to the proportion of health states within risk groups and among individuals moving between risk groups, respectively. However, circle sizes and arrow widths do not have comparable scales. Appendix Figure C.1 illustrates proportions of health states versus turnover in full.

Therefore, the inverted U-shaped relationship between turnover rate and equilibrium STI prevalence in the high risk group was mediated by the combination of the above three phenomena. When systems moved from no turnover to slow turnover, reduction in herd immunity (phenomenon 2) predominated, leading to increasing equilibrium prevalence with turnover (Figure 4a, region A). When systems were modelled under faster and faster turnover, outflow of infectious individuals from the group via turnover (phenomenon 1) and reduction in the average number of partners per year among infectious individuals (phenomenon 3) predominated, leading to lower equilibrium prevalence at faster rates of turnover (Figure 4a, region B).

3.1.2. Influence of turnover on equilibrium prevalence in the low risk group

As shown in Figure 6, at equilibrium, the low risk group was composed mainly of susceptible individuals. Moving from a system no turnover to one with slow turnover lead to a net inflow of infectious and treated individuals (Figures 5e and 5f, yellow), and a net removal of susceptible individuals (Figure 5d, yellow). The net inflow of infectious individuals (Figure 5e, yellow) contributed to higher equilibrium prevalence in the
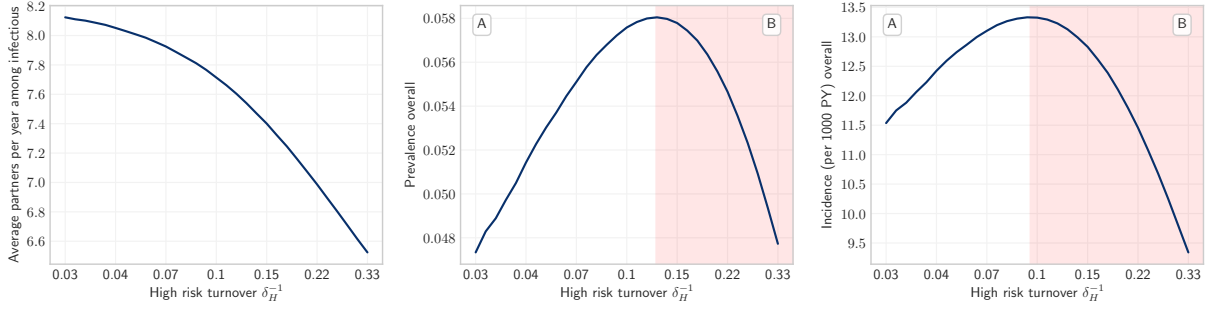
(a) Average number of partners per year among infectious individuals

(b) Overall prevalence

(c) Overall incidence

Figure 7: Overall incidence and the non-constant factors of incidence versus turnover. The product of factors (a) and (b) is proportional to (c) overall incidence. See Appendix B.4 for proof.

Turnover rate (log scale) is a function of the duration of time spent in the high risk group δ_H, where shorter time spent in the high risk group yields faster turnover. No turnover is indicated by $\delta_H^{-1} = 0.03$, due to population exit rate $\mu = 0.03$.

low risk group when the system moved from no turnover to slow turnover (phenomenon 1). The inflow of infectious and treated individuals only slightly reduced the already large proportion who were susceptible in the low risk group. Thus, there was little increase in herd immunity within the low risk group as turnover increased (phenomenon 2). However, incident infections still rose in the low risk group as the system moved from no turnover to slow turnover (Figure 5e, red) due to higher incidence in the total population (Figure 7c) which was largely driven by reduced herd immunity in the high risk group (see Section 3.1.1; phenomenon 2). Under faster rates of turnover, incident infections declined in the low risk group (Figure 5e, red) due to lower incidence in the total population (Figure 7c) which was driven by decreasing number of partners per year among infectious individuals (Figure 7a; phenomenon 3), as described in Section 3.1.1.

Therefore, as in the high risk group, the inverted U-shaped relationship between turnover rate and equilibrium STI prevalence in the low risk group was mediated by the combination of the above three phenomena. Moving from no turnover to slow turnover, the net inflow of infectious individuals (phenomenon 1) and reduced herd immunity in the high risk group (phenomenon 2) predominated, leading to higher equilibrium prevalence (Figure 4c, region A). At higher rates of turnover, a decreasing overall incidence due to a reduction in the number of partners among infectious individuals (phenomenon 3) predominated, leading to declining equilibrium prevalence (Figure 4c, region B).

In sum, there were three phenomena that drove shifts in equilibrium STI prevalence across risk groups at variable rates of turnover: 1) net flows of infectious individuals from high risk groups into low risk groups; 2) changes to herd immunity, especially within the high risk group; and 3) changes to the number of partnerships available with infectious individuals.
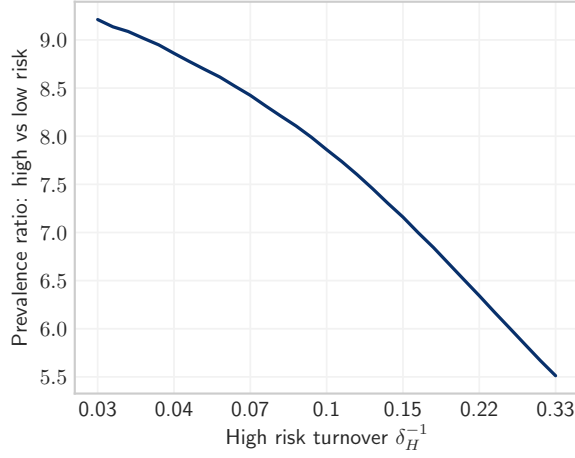
Figure 8: Equilibrium prevalence ratios between high and low risk groups under different rates of turnover. Turnover rate (log scale) is a function of the duration of time spent in the high risk group δ_H, where shorter time spent in the high risk group yields faster turnover. No turnover is indicated by $\delta_H^{-1} = 0.03$, due to population exit rate $\mu = 0.03$.

3.1.3. Influence of turnover on STI prevalence ratio between high and low risk groups

As discussed in Sections 3.1.1 and 3.1.2, turnover caused a net outflow of infectious individuals from the high risk group (Figure 5b, yellow) and a net inflow of infectious individuals into the low risk group (Figure 5e, yellow). In contrast, the influence of turnover on the rate of incident infections followed a more similar pattern in both the high and low risk groups (Figures 5b and 5e, red). Therefore, differences in the influence of turnover on prevalence between risk groups were driven by net movement of infectious individuals from high to low risk, causing prevalence in the high and low risk groups to come closer together with faster turnover. As shown in Figure 8, the ratio of equilibrium STI prevalence in the high versus low risk groups was thus reduced under faster turnover rates. For example, the prevalence ratio between high and low risk groups was: 6.7 in the model under high turnover ($\delta_H = 5$ years) versus 9.2 in the model without turnover ($\delta_H = 33$ years) (Table 3). Finally, the propensity for equilibrium STI prevalence to decrease in the high risk group and for prevalence to increase in the low risk group with faster turnover (due to net movement of infectious individuals from high to low risk) also explains why prevalence peaked at slower turnover in the high risk group (Figure 4a) and faster turnover in the low risk group (Figure 4c).

3.2. Experiment 2: Inferred risk heterogeneity with versus without turnover

After model fitting, our two STI transmission models (one with turnover and one without turnover) reproduced the target equilibrium STI prevalence values of 20%, 8.75%, 3%, and 5% in the high, medium, low risk groups, and total population, respectively (Table 3; Figure C.7). When fitting the model with turnover to these group-specific prevalence targets, the fitted numbers of partners per year C_i (the only non-fixed parameter) had to compensate for the reduction in STI prevalence ratio between high and low

Table 3: Equilibrium partnership formation rates and prevalence among the high and low risk groups predicted by the models with and without turnover, before and after model fitting.

	Number of Partners			Prevalence		
Context	High	Low	High/Low	High	Low	High/Low
Turnover	25.0	1.0	25.0	21.6%	3.2%	**6.7**
No Turnover	25.0	1.0	25.0	21.9%	2.4%	**9.2**
Turnover [fit]	24.3	1.0	**23.9**	20.0%	3.0%	6.7
No Turnover [fit]	23.5	1.5	**15.2**	20.0%	3.0%	6.7

risk groups (Figure 8). As a result, the ratio of fitted partner numbers between high and low risk groups (C_H / C_L) had to be higher in the model with turnover compared to the model without turnover: 23.9 vs 15.2 (Table 3). That is, the inferred level of risk heterogeneity was higher in the model with turnover than in the model without turnover.

3.3. Experiment 3: Influence of turnover on the tPAF of the high risk group

Finally, we compared the tPAF of the high risk group projected by the fitted model with turnover and the fitted model without turnover (Figure 9). The tPAF projected by both models increased over longer and longer time horizons, indicating that unmet prevention and treatment needs of the high risk group were central to epidemic persistence in both fitted models. The model with turnover projected a larger tPAF at all time-horizons compared with the tPAF projected by the model without turnover. The larger tPAF projected by the model with turnover stemmed from more risk heterogeneity (Table 3) which led to more onward transmission from the unmet prevention and treatment needs of the high risk group.

4. Discussion

Using a mechanistic modelling analysis, we found that turnover could be important when projecting the tPAF of high risk groups to the overall epidemic. Mechanistic insights include disentangling three key phenomena by which turnover alters equilibrium STI prevalence within risk groups, and thereby the level of inferred risk heterogeneity between groups via model fitting. Methodological contributions include a framework for modelling turnover which uses a flexible combination of data-driven constraints. Taken together, our explanatory insights and framework have mechanistic, public health, and methodological relevance for the parameterization and use of epidemic models to project intervention priorities for high risk groups.

Influence of turnover on prevalence. Building on prior work by Stigum et al. (1994); Zhang et al. (2012); Henry and Koopman (2015) which similarly found an inverted U-shaped relationship between turnover and
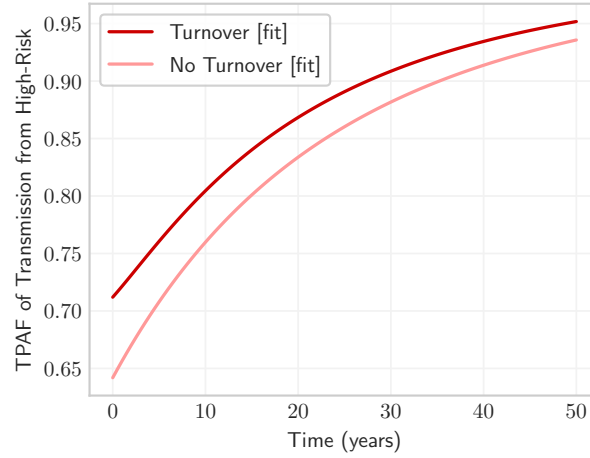
14

Figure 9: Transmission population attributable fraction (tPAF) of the high risk group in models with and without turnover, after fitting the number of partners per year to group-specific prevalence.

overall equilibrium STI prevalence, we identified three key phenomena that generated this relationship. These turnover-driven phenomena were: 1) a net flow of infectious individuals from higher risk groups to lower risk groups; 2) reduced herd immunity in the higher risk groups due to net gain of susceptible individuals; and 3) reduced incidence overall due to fewer partner numbers among infectious individuals. The above three phenomena contributed to the pattern of declining prevalence ratio between the highest and lowest risk groups for increasing rates of turnover. A decline in prevalence ratio due to turnover implies a reduction in risk heterogeneity. Since risk heterogeneity is associated with epidemic emergence and persistence (May and Anderson, 1988) – i.e. the basic reproductive number – our findings are thus consistent with Henry and Koopman (2015), who demonstrated that turnover reduces the basic reproductive number by reducing heterogeneity. Indeed, epidemiological and transmission modelling studies have shown that prevalence ratios are an important marker of risk heterogeneity, and in turn the impact of interventions focused on high risk groups (Baral et al., 2012; Mishra et al., 2012).

Implications for interventions. Our comparison of fitted models with and without turnover showed that if turnover exists in a given setting but is ignored in a model, the inferred heterogeneity in risk would be lower than in reality, while reproducing the same STI prevalence in each risk group. As a result, the projected tPAF of high risk groups could be systematically underestimated by models that ignore turnover. Although we examined a single parameter to capture risk (number of partners per year), the findings would hold for any combination of factors that alter the risk per susceptible individual (force of infection), including biological transmission probabilities and rates of partner change (Anderson and May, 1991). The public health implications of models ignoring turnover, and thereby underestimating risk heterogeneity and the tPAF of high risk groups, is that resources could potentially be misguided away from high risk groups.

15

For example, epidemic models which fail to include or accurately capture turnover may underestimate the importance of addressing the unmet needs of key populations at disproportionate risk of HIV and other STIs, such as gay men and other men who have sex with men, transgender women, people who use drugs, and sex workers. In many HIV epidemic models of regions with high HIV prevalence, such as in Southern Africa, key populations have historically been subsumed into the overall modelled population; which meant, by design, less risk heterogeneity (Eaton et al., 2012; Cori et al., 2014; Mishra et al., 2016). Our findings suggest that even when key populations are included, it is important to further capture within-person changes in risks over time (such as duration in sex work). Underestimating risk heterogeneity could also underestimate the resources required to achieve local epidemic control, as suggested by Henry and Koopman (2015); Hontelez et al. (2013). Important next steps surrounding the potential bias in tPAF projections attributable to inclusion/exclusion of turnover include quantifying the magnitude of bias, and characterizing the epidemiologic conditions under which the bias would be meaningfully large in the context of public health programmes.

Turnover framework. We developed a unified framework to parameterize risk group turnover using available epidemiologic data and/or assumptions. There are four potential benefits of using the framework to model turnover. First, the framework defines how specific epidemiologic data and assumptions could be used as constraints to help define rates of turnover. Second, the framework allows flexibility in which constraints can be chosen and combined, so that the constraints best reflect locally available data and/or plausible assumptions. In fact, the framework can adequately reproduce several prior implementations of turnover in various epidemic models (Stigum et al., 1994; Eaton and Hallett, 2014; Henry and Koopman, 2015). Third, this flexible approach also allows the framework to scale to any number of risk groups. Finally, the framework avoids the need for a burn-in period to establish a demographic steady-state before introducing infection, which was required in some previous models (Boily et al., 2015).

As noted above, one benefit of the unified framework for modelling turnover is clarifying data priorities for parameterizing turnover. Absolute or relative population size estimates across risk groups may be obtained from population-based sexual behaviour surveys (The DHS Program, 2019), and from mapping and enumeration of marginalized persons such as sex workers (Abdul-Quader et al., 2014). The proportion of individuals who enter into each risk group may be available through sexual behaviour surveys: for example, among individuals who became sexually active for the first time in the past year, the proportion who also engaged in multiple partnerships within the past year. The average duration of time spent within each risk group, such as the duration in sex work, may be drawn from cross-sectional survey questions such as "for how many years have you been a sex worker?" albeit with the recognition that such data are censored (Watts et al., 2010). Longitudinal, or cohort studies that track self-reported sexual behaviour over time can also provide estimates of duration of time spent within a given risk strata (Fergus et al., 2007), or provide

16

direct estimates of transition rates between risk strata.

Limitations. Our framework for modelling turnover was developed specifically to answer mechanistic questions about the tPAF; as such, there are two key limitations of the framework in its current form. First, the framework did not stratify the population by sex or age. In the context of real-world STI epidemics, the relative size of risk groups may differ by both sex and age, such as the often smaller number of females and/or males who sell sex, versus the larger number of males who pay for sex (clients of female or male sex workers). Second, the framework does not account for infection-attributable mortality, such as HIV-attributable mortality. However, modelling studies have shown that HIV-attributable mortality can reduce the relative size of higher risk groups who bear a disproportionate burden of HIV, which in turn can cause an HIV epidemic to decline (Boily and Mâsse, 1997). As such, many models of HIV transmission that include very small ($< 3\%$ of the population) high risk groups, such as female sex workers, often do not constrain the relative size of the sub-group populations to be stable over time (Pickles et al., 2013). By ignoring infection-attributable mortality, the proposed framework would similarly allow risk groups to change relative size in response to disproportionate infection-attributable mortality. Future modifications of the proposed framework include methods to optionally re-balance infection-attributable mortality, and relevant age-sex stratifications so that the framework can be applied more broadly to pathogen-specific epidemics.

Our analyses of turnover and tPAF also have several limitations. First, we did not capture the possibility that some individuals may become re-susceptible to infection after treatment – an important feature of many STIs such as syphilis and gonorrhoea (Fenton et al., 2008). As shown by Fenton et al. (2008) and Pourbohloul et al. (2003), the re-supply of susceptible individuals following STI treatment could fuel an epidemic, and so the influence of turnover on STI prevalence and tPAF may be different. Second, our analyses were restricted to equilibrium STI prevalence. The influence of turnover on prevalence and tPAF may vary within different phases of an epidemic – growth, mature, declining (Wasserheit and Aral, 1996). Finally, our analyses reflected an illustrative STI epidemic in a population with illustrative risk strata. Important next steps in the examination of the extent to which turnover influences the tPAF include pathogen- and population-specific modelling – such as the comparisons of model structures by Hontelez et al. (2013); Johnson and Geffen (2016) – and at different epidemic phases.

Conclusion. In conclusion, turnover may influence prevalence of infection, and thus influence inference on risk heterogeneity when fitting risk-stratified epidemic models. If models do not capture turnover, the projected contribution of high risk groups, and thus, the potential impact of prioritizing interventions to meet their needs, could be underestimated. To aid the next generation of epidemic models used to estimate the tPAF of high risk groups – including key populations – data collection efforts to parameterize risk group turnover should be prioritized.

Acknowledgements

Contributions

JK and SM conceptualized the study and drafted the manuscript; JK designed the experiments with input from LW, HM, and SM. JK developed the unified framework and conducted the modelling, experiments, and analyses; conducted the literature review, and drafted the first version of the manuscript. LW, HM, SB, and SS led substantial structural revisions to the manuscript, including assessment of epidemiological constraints and assumptions; and provided critical discussion surrounding implications of findings. All authors contributed to interpretation of the results and manuscript revision.

Funding

Conflicts of Interest

Declarations of interest: none.

References

Abdul-Quader, A.S., Baughman, A.L., Hladik, W., 2014. Estimating the size of key populations: Current status and future possibilities 9, 107–114. doi:10.1097/COH.0000000000000041.

Anderson, R.M., May, R.M., 1991. Infectious diseases of humans: dynamics and control. Infectious diseases of humans: dynamics and control. .

Baral, S., Beyrer, C., Muessig, K., Poteat, T., Wirtz, A.L., Decker, M.R., Sherman, S.G., Kerrigan, D., 2012. Burden of HIV among female sex workers in low-income and middle-income countries: A systematic review and meta-analysis. The Lancet Infectious Diseases 12, 538–549. URL: https://www.sciencedirect.com/science/article/pii/S147330991270066X?via{%}3Dihub, doi:10.1016/S1473-3099(12)70066-X.

Baral, S., Ketende, S., Green, J.L., Chen, P.A.A., Grosso, A., Sithole, B., Ntshangase, C., Yam, E., Kerrigan, D., Kennedy, C.E., Adams, D., 2014. Reconceptualizing the HIV epidemiology and prevention needs of female sex workers (FSW) in Swaziland. PLoS ONE 9, e115465. doi:10.1371/journal.pone.0115465.

Baral, S., Logie, C.H., Grosso, A., Wirtz, A.L., Beyrer, C., 2013. Modified social ecological model: A tool to guide the assessment of the risks and risk contexts of HIV epidemics. BMC Public Health 13, 482. doi:10.1186/1471-2458-13-482.

Boily, M.C., Mâsse, B., 1997. Mathematical models of disease transmission: A precious tool for the study of sexually transmitted diseases. Canadian Journal of Public Health 88, 255–265. doi:10.1007/bf03404793.

Boily, M.C., Pickles, M., Alary, M., Baral, S., Blanchard, J., Moses, S., Vickerman, P., Mishra, S., 2015. What really is a concentrated HIV epidemic and what does it mean for West and Central Africa? Insights from mathematical modeling. Journal of Acquired Immune Deficiency Syndromes 68, S74–S82. doi:10.1097/QAI.0000000000000437.

Case, K., Ghys, P., Gouws, E., Eaton, J., Borquez, A., Stover, J., Cuchi, P., Abu-Raddad, L., Garnett, G., Hallett, T., 2012. Understanding the modes of tranmission model of new HIV infection and its use in prevention planning. Bulletin of the World Health Organization 90, 831–838. doi:10.2471/blt.12.102574.

Cori, A., Ayles, H., Beyers, N., Schaap, A., Floyd, S., Sabapathy, K., Eaton, J.W., Hauck, K., Smith, P., Griffith, S., Moore, A., Donnell, D., Vermund, S.H., Fidler, S., Hayes, R., Fraser, C., 2014. HPTN 071 (PopART): A cluster-randomized trial of the population impact of an HIV combination prevention intervention including universal testing and treatment: Mathematical model. PLoS ONE 9, e84511. URL: https://dx.plos.org/10.1371/journal.pone.0084511, doi:10.1371/journal.pone.0084511.

DataBank, 2019. Population estimates and projections. URL: https://databank.worldbank.org/source/population-estimates-and-projections.

Eaton, J.W., Hallett, T.B., 2014. Why the proportion of transmission during early-stage HIV infection does not predict the long-term impact of treatment on HIV incidence. Proceedings of the National Academy of Sciences 111, 16202–16207. doi:10.1073/pnas.1323007111.

Eaton, J.W., Johnson, L.F., Salomon, J.A., Bärnighausen, T., Bendavid, E., Bershteyn, A., Bloom, D.E., Cambiano, V., Fraser, C., Hontelez, J.A., Humair, S., Klein, D.J., Long, E.F., Phillips, A.N., Pretorius, C., Stover, J., Wenger, E.A., Williams, B.G., Hallett, T.B., 2012. HIV treatment as prevention: Systematic comparison of mathematical models of the potential impact of antiretroviral therapy on HIV incidence in South Africa. PLoS Medicine 9, e1001245. URL: https://dx.plos.org/10.1371/journal.pmed.1001245, doi:10.1371/journal.pmed.1001245.

Fenton, K.A., Breban, R., Vardavas, R., Okano, J.T., Martin, T., Aral, S., Blower, S., 2008. Infectious syphilis in high-income settings in the 21st century. The Lancet Infectious Diseases 8, 244–253. doi:10.1016/S1473-3099(08)70065-3.

Fergus, S., Zimmerman, M.A., Caldwell, C.H., 2007. Growth trajectories of sexual risk behavior in adolescence and young adulthood. American Journal of Public Health 97, 1096–1101. doi:10.2105/AJPH.2005.074609.

Ganem, D., Prince, A.M., 2004. Hepatitis B Virus Infection — Natural History and Clinical Consequences. New England Journal of Medicine 350, 1118–1129. doi:10.1056/NEJMra031087.

Garnett, G.P., Anderson, R.M., 1994. Balancing sexual partnership in an age and activity stratified model of HIV transmission in heterosexual populations. Mathematical Medicine and Biology 11, 161–192. doi:10.1093/imammb/11.3.161.

Hanley, J.A., 2001. A heuristic approach to the formulas for population attributable fraction. Journal of Epidemiology and Community Health 55, 508–514. doi:10.1136/jech.55.7.508.

Henry, C.J., Koopman, J.S., 2015. Strong influence of behavioral dynamics on the ability of testing and treating HIV to stop transmission. Scientific Reports 5, 9467. doi:10.1038/srep09467.

Hontelez, J.A.C., Lurie, M.N., Bärnighausen, T., Bakker, R., Baltussen, R., Tanser, F., Hallett, T.B., Newell, M.L., de Vlas, S.J., 2013. Elimination of HIV in South Africa through Expanded Access to Antiretroviral Therapy: A Model Comparison Study. PLoS Medicine 10, e1001534. URL: http://dx.plos.org/10.1371/journal.pmed.1001534, doi:10.1371/journal.pmed.1001534.

ICAP, 2019. PHIA Project. URL: https://phia.icap.columbia.edu.

Johnson, L.F., Geffen, N., 2016. A Comparison of two mathematical modeling frameworks for evaluating sexually transmitted infection epidemiology. Sexually Transmitted Diseases 43, 139–146. doi:10.1097/OLQ.0000000000000412.

Knight, J., Wang, L., Ma, H., Schwartz, S., Baral, S., Mishra, S., 2019. The influence of risk group turnover in STI/HIV epidemics: mechanistic insights from transmission modeling, in: STI & HIV 2019 World Congress, Vancouver, BC, Canada. URL: https://sti.bmj.com/content/95/Suppl_1/A83.3.

Koopman, J.S., Jacquez, J.A., Welch, G.W., Simon, C.P., Foxman, B., Pollock, S.M., Barth-Jones, D., Adams, A.L., Lange, K., 1997. The role of early HIV infection in the spread of HIV through populations. Journal of Acquired Immune Deficiency Syndromes 14, 249–58. URL: http://www.ncbi.nlm.nih.gov/pubmed/9117458.

Kraft, D., 1988. A software package for sequential quadratic programming. Technical Report DFVLR-FB 88-28. DLR German Aerospace Center — Institute for Flight Mechanics. Koln, Germany.

LAPACK, 1992. LAPACK: Linear Algebra PACKage. URL: http://www.netlib.org/lapack.

Lawson, C.L., Hanson, R.J., 1995. Solving least squares problems. volume 15. SIAM.

Maartens, G., Celum, C., Lewin, S.R., 2014. HIV infection: Epidemiology, pathogenesis, treatment, and prevention. The Lancet 384, 258–271. doi:10.1016/S0140-6736(14)60164-1.

Maheu-Giroux, M., Vesga, J.F., Diabaté, S., Alary, M., Baral, S., Diouf, D., Abo, K., Boily, M.C., 2017. Changing Dynamics of HIV Transmission in Côte d'Ivoire: Modeling Who Acquired and Transmitted Infections and Estimating the Impact of Past HIV Interventions (1976-2015). Journal of Acquired Immune Deficiency Syndromes 75, 517–527. doi:10.1097/QAI.0000000000001434.

Malthus, T.R., 1798. An Essay on the Principle of Population.

Marston, C., King, E., 2006. Factors that shape young people's sexual behaviour: a systematic review. Lancet 368, 1581–1586. doi:10.1016/S0140-6736(06)69662-1.

May, R.M., Anderson, R.M., 1988. The transmission dynamics of human immunodeficiency virus (HIV). doi:10.1098/rstb.1988.0108.

Mishra, S., Boily, M.C., Schwartz, S., Beyrer, C., Blanchard, J.F., Moses, S., Castor, D., Phaswana-Mafuya, N., Vickerman, P., Drame, F., Alary, M., Baral, S.D., 2016. Data and methods to characterize the role of sex work and to inform sex work programs in generalized HIV epidemics: evidence to challenge assumptions. Annals of Epidemiology 26, 557–569. doi:10.1016/j.annepidem.2016.06.004.

Mishra, S., Pickles, M., Blanchard, J.F., Moses, S., Boily, M.C., 2014. Distinguishing sources of HIV transmission from the distribution of newly acquired HIV infections: Why is it important for HIV prevention planning? Sexually Transmitted Infections 90, 19–25. doi:10.1136/sextrans-2013-051250.

Mishra, S., Steen, R., Gerbase, A., Lo, Y.R., Boily, M.C., 2012. Impact of High-Risk Sex and Focused Interventions in Heterosexual HIV Epidemics: A Systematic Review of Mathematical Models. PLoS ONE 7, e50691. doi:10.1371/journal.

pone.0050691.

Mukandavire, C., Walker, J., Schwartz, S., Boily, M.C., Danon, L., Lyons, C., Diouf, D., Liestman, B., Diouf, N.L., Drame, F., Coly, K., Muhire, R.S.M., Thiam, S., Diallo, P.A.N., Kane, C.T., Ndour, C., Volz, E., Mishra, S., Baral, S., Vickerman, P., 2018. Estimating the contribution of key populations towards the spread of HIV in Dakar, Senegal. Journal of the International AIDS Society 21, e25126. doi:10.1002/jia2.25126.

Pickles, M., Boily, M.C., Vickerman, P., Lowndes, C.M., Moses, S., Blanchard, J.F., Deering, K.N., Bradley, J., Ramesh, B.M., Washington, R., Adhikary, R., Mainkar, M., Paranjape, R.S., Alary, M., 2013. Assessment of the population-level effectiveness of the Avahan HIV-prevention programme in South India: A preplanned, causal-pathway-based modelling analysis. The Lancet Global Health 1, e289–e299. doi:10.1016/S2214-109X(13)70083-4.

Pourbohloul, B., Rekart, M.L., Brunham, R.C., 2003. Impact of mass treatment on syphilis transmission: A mathematical modeling approach. Sexually Transmitted Diseases 30, 297–305. doi:10.1097/00007435-200304000-00005.

Prüss-Ustün, A., Wolf, J., Driscoll, T., Degenhardt, L., Neira, M., Calleja, J.M.G., 2013. HIV Due to Female Sex Work: Regional and Global Estimates. PLoS ONE 8, e63476. doi:10.1371/journal.pone.0063476.

Shubber, Z., Mishra, S., Vesga, J.F., Boily, M.C., 2014. The HIV modes of transmission model: A systematic review of its findings and adherence to guidelines. Journal of the International AIDS Society 17, 18928. doi:10.7448/IAS.17.1.18928.

Stigum, H., Falck, W., Magnus, P., 1994. The core group revisited: The effect of partner mixing and migration on the spread of gonorrhea, chlamydia, and HIV. Mathematical Biosciences 120, 1–23. doi:10.1016/0025-5564(94)90036-1.

The DHS Program, 2019. Data. URL: https://www.dhsprogram.com.

Wasserheit, J.N., Aral, S.O., 1996. The Dynamic Topology Of Sexually Transmitted Disease Epidemics: Implications For Prevention Strategies. Journal of Infectious Diseases 174, S201–S213. URL: https://academic.oup.com/jid/article-lookup/doi/10.1093/infdis/174.Supplement{_}2.S201, doi:10.1109/ICPDS.2016.7756727.

Watts, C., Zimmerman, C., Foss, A.M., Hossain, M., Cox, A., Vickerman, P., 2010. Remodelling core group theory: the role of sustaining populations in HIV transmission. Sexually Transmitted Infections 86, iii85–iii92. doi:10.1136/sti.2010.044602.

Yorke, J.A., Hethcote, H.W., Nold, A., 1978. Dynamics and control of the transmission of gonorrhea. Sexually Transmitted Diseases 5, 51–56. doi:10.1097/00007435-197804000-00003.

Zhang, X., Zhong, L., Romero-Severson, E., Alam, S.J., Henry, C.J., Volz, E.M., Koopman, J.S., 2012. Episodic HIV Risk Behavior Can Greatly Amplify HIV Prevalence and the Fraction of Transmissions from Acute HIV Infection. Statistical Communications in Infectious Diseases 4. doi:10.1515/1948-4690.1041.

A. Turnover Framework

We introduce a system of parameters and constraints to describe risk group turnover in deterministic epidemic models with heterogeneity in risk.[1] We then describe how the system can be used in practical terms, based on different assumptions and data available for parameterizing turnover in risk. We conclude by framing previous approaches to this task using the proposed system.

A.1. Notation

Consider a population divided into G risk groups. We denote the number of individuals in risk group $i \in [1, \ldots, G]$ as x_i and the set of all risk groups as $\boldsymbol{x} = \{x_1, \ldots, x_G\}$. The total population size is $N = \sum_i x_i$, and the relative population size of each group is denoted as $\hat{x}_i = x_i/N$. Individuals enter the population at a rate ν per year, and exit at a rate μ per year. We model the distribution of risk groups among individuals entering into the population as $\hat{\boldsymbol{e}}$, which may be different from individuals already in the population $\hat{\boldsymbol{x}}$.[2] Thus, the total number of individuals entering into population $\boldsymbol{x}$ per year is given by νN, and the number of individuals entering into group i specifically is given by $\hat{e}_i \nu N$.

Turnover transitions may then occur between any two groups, in either direction. Therefore we denote the turnover rates as a $G \times G$ matrix ϕ. The element ϕ_{ij} corresponds to the proportion of individuals in group i who move from group i to group j each year. An example matrix is given in Eq. (A.1), where we write the diagonal elements as $*$ since they represent transitions from a group to itself.

$$
\phi = \begin{bmatrix}
* & x_1 \to x_2 & \cdots & x_1 \to x_G \\
x_2 \to x_1 & * & \cdots & x_2 \to x_G \\
\vdots & \vdots & \ddots & \vdots \\
x_G \to x_1 & x_G \to x_2 & \cdots & *
\end{bmatrix}
\tag{A.1}
$$

Risk groups, transitions, and the associated rates are also shown for $G = 3$ in Figure A.1.

A.2. Parameterization

Next, we present methods to illustrate how epidemiologic data can be used to parametrize turnover in epidemic models. We construct a system like the one above which reflects the risk group dynamics observed in a specific context. We assume that the relative sizes of the risk groups in the model ($\hat{\boldsymbol{x}}$) are already known, and should remain constant over time. Thus, what remains is to estimate the values of the parameters: ν, μ, $\hat{\boldsymbol{e}}$, and ϕ, using commonly available sources of data.

---

[1] A preliminary version of this framework was used by Knight et al. (2019).

[2] We could equivalently stratify the rate of entry ν by risk group; however, we find that the mathematics in subsequent sections are more straightforward using $\hat{\boldsymbol{e}}$.
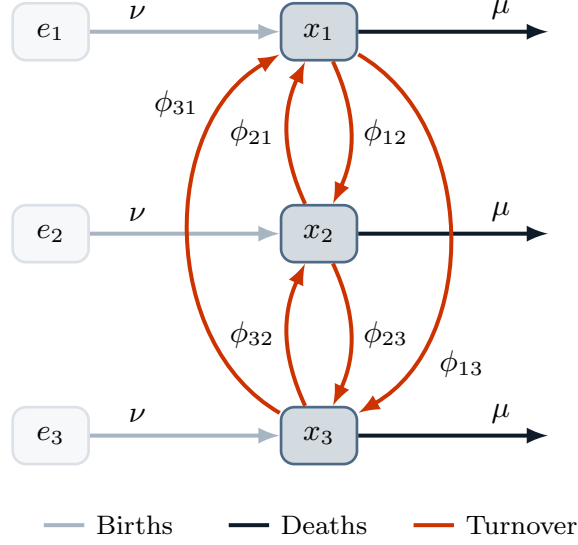
Figure A.1: System of $G = 3$ risk groups and turnover between them.
x_i: number of individuals in risk group i; e_i: number of individuals available to enter risk group i; ν: rate of population entry; μ: rate of population exit; ϕ_{ij}: rate of turnover from group i to group j.

A.2.1. Total Population Size

The total population size $N(t)$ is a function of the rates of population entry $\nu(t)$ and exit $\mu(t)$, given an initial size N_0. We allow the proportion entering the system to vary by risk group via $\hat{\boldsymbol{e}}$, while the exit rate has the same value for each group. We assume that there is no disease-attributable death. Because the values of ν and μ are the same for each risk group, they can be estimated independent of $\hat{\boldsymbol{x}}$, $\hat{\boldsymbol{e}}$, and ϕ.

The difference between entry and exit rates defines the rate of population growth:

$$\mathcal{G}(t) = \nu(t) - \mu(t) \tag{A.2}$$

The total population may then be defined using an initial population size N_0 as:

$$N(t) = N_0 \exp\left(\int_0^t \log\left(1 + \mathcal{G}(\tau)\right)d\tau\right) \tag{A.3}$$

which, for constant growth, simplifies to the familiar expression (Malthus, 1798):

$$N(t) = N_0(1 + \mathcal{G})^t \tag{A.4}$$

Census data, such as (DataBank, 2019), can be used to source the total population size in a given geographic setting over time $N(t)$, thus allowing Eqs. (A.3) and (A.4) to be used to estimate $\mathcal{G}(t)$.

If the population size is assumed to be constant, then $\mathcal{G}(t) = 0$ and $\nu(t) = \mu(t)$. If population growth occurs at a stable rate, then $\mathcal{G}$ is fixed at a constant value which can be estimated via Eq. (A.4) using any

two values of $N(t)$, separated by a time interval τ:

$$\mathcal{G}_\tau = \frac{N(t+\tau)^{\frac{1}{\tau}}}{N(t)} - 1 \tag{A.5}$$

If the rate of population growth $\mathcal{G}$ varies over time, then Eq. (A.5) can be reused for consecutive time intervals, and the complete function $\mathcal{G}(t)$ approximated piecewise by constant values. The piecewise approximation can be more feasible than exact solutions using Eq. (A.3), and can reproduce $N(t)$ accurately for small enough intervals τ, such as one year.

Now, given a value of $\mathcal{G}(t)$, either $\nu(t)$ must be chosen and $\mu(t)$ calculated using Eq. (A.2), or $\mu(t)$ must be chosen, and $\nu(t)$ calculated. Most modelled systems assume a constant duration of time that individuals spend in the model $\delta(t)$ (Anderson and May, 1991) which is related to the rate of exit μ by:

$$\delta(t) = \mu^{-1}(t) \tag{A.6}$$

In the context of sexually transmitted infections, the duration of time usually reflects the average sexual life-course of individuals from age 15 to 50 years, such that $\delta = 35$ years. The duration δ may also vary with time to reflect changes in life expectancy. The exit rate $\mu(t)$ can then be defined as $\delta^{-t}(t)$ following Eq. (A.6), and the entry rate $\nu(t)$ defined as $\mathcal{G}(t) - \mu(t)$ following Eq. (A.2).

A.2.2. Turnover

Next, we present methods for resolving the distribution of individuals entering the risk model $\hat{\boldsymbol{e}}(t)$ and the rates of turnover $\phi(t)$, assuming that entry and exit rates $\nu(t)$ and $\mu(t)$ are known. Similar to above, we first formulate the problem as a system of equations. Then, we explore the data and assumptions required to solve for the values of parameters in the system. The (t) notation is omitted throughout this section for clarity, though time-varying parameters can be estimated by repeating the necessary calculations for each t.

The number of risk groups G dictates the number of unknown elements in $\hat{\boldsymbol{e}}$ and ϕ: G and $G(G-1)$, respectively. We collect these unknowns in the vector $\boldsymbol{\theta} = [\hat{\boldsymbol{e}}, \boldsymbol{y}]$, where $\boldsymbol{y} = \text{vec}_{i \neq j}(\phi)$. For example, for $G = 3$, the vector $\boldsymbol{\theta}$ is defined as:

$$\boldsymbol{\theta} = \left[\begin{array}{ccccccccc} \hat{e}_1 & \hat{e}_2 & \hat{e}_3 & \phi_{12} & \phi_{13} & \phi_{21} & \phi_{23} & \phi_{31} & \phi_{32} \end{array} \right] \tag{A.7}$$

We then define a linear system of equations which uniquely determine the elements of $\boldsymbol{\theta}$:

$$\boldsymbol{b} = A\,\boldsymbol{\theta} \tag{A.8}$$

where A is a $M \times G^2$ matrix and $\boldsymbol{b}$ is a M-length vector. Specifically, each row in A and $\boldsymbol{b}$ defines a constraint: an assumed mathematical relationship involving one or more elements of $\hat{\boldsymbol{e}}$ and ϕ. For example, a simple constraint could be to assume the value $\hat{e}_2 = 0.20$. Each of the following four sections introduces a type of constraint, including: assuming a constant group size, specifying elements of $\boldsymbol{\theta}$ directly, assuming an average

duration in a group, and specifying a relationship between two individual rates of turnover. Constraints may be selected and combined together based on availability of data and plausibility of assumptions. However, a total of $M = G^2$ constraints must be defined in order to obtain a "unique solution": exactly one value of $\boldsymbol{\theta}$ which satisfies all constraints. The values of $\hat{\boldsymbol{e}}$ and ϕ can then be calculated algebraically by solving Eq. (A.8) with $\boldsymbol{\theta} = A^{-1}\boldsymbol{b}$, for which many algorithms exist (LAPACK, 1992).

1. Constant group size. One epidemiologic feature that epidemic models consider is whether or not the relative sizes of risk groups are constant over time (Henry and Koopman, 2015; Boily et al., 2015). Assuming constant group size implies a stable level of heterogeneity over time. To enforce this assumption, we define the "conservation of mass" equation for group i, wherein the rate of change of the group is defined as the sum of flows in / out of the group:

$$\frac{d}{dt}x_i = \nu N\hat{e}_i + \sum_j \phi_{ji}\,x_j - \mu\,x_i - \sum_j \phi_{ij}\,x_i \tag{A.9}$$

Eq. (A.9) is written in terms of absolute population sizes $\boldsymbol{x}$, but can be written as proportions $\hat{\boldsymbol{x}}$ by dividing all terms by N. If we assume that the proportion of each group $\hat{x}_i$ is constant over time, then the desired rate of change for risk group i will be equal to the rate of population growth of the risk group, $\mathcal{G}x_i$. Substituting $\frac{d}{dt}x_i = \mathcal{G}x_i$ into Eq. (A.9), and simplifying yields:

$$\nu\,x_i = \nu\,N\hat{e}_i + \sum_j \phi_{ji}\,x_j - \sum_j \phi_{ij}\,x_i \tag{A.10}$$

Factoring the left and right hand sides in terms of $\hat{\boldsymbol{e}}$ and ϕ, we obtain G unique constraints. For $G = 3$, this yields the following 3 rows as the basis of $\boldsymbol{b}$ and A:

$$\boldsymbol{b} = \begin{bmatrix} \nu x_1 \\ \nu x_2 \\ \nu x_3 \end{bmatrix}; \qquad A = \begin{bmatrix} \nu & \cdot & \cdot & -x_1 & -x_1 & x_2 & \cdot & x_3 & \cdot \\ \cdot & \nu & \cdot & x_1 & \cdot & -x_2 & -x_2 & \cdot & x_3 \\ \cdot & \cdot & \nu & \cdot & x_1 & \cdot & x_2 & -x_3 & -x_3 \end{bmatrix} \tag{A.11}$$

These G constraints ensure risk groups do not change size over time. However, a unique solution requires an additional $G(G-1)$ constraints. For $G = 3$, this corresponds to 6 additional constraints.

2. Specified elements. The simplest type of additional constraint is to directly specify the values of individual elements in $\hat{\boldsymbol{e}}$ or ϕ. Such constraints may be appended to $\boldsymbol{b}$ and A as an additional row k using indicator notation.[3] That is, with b_k as the specified value v, and A_k as the indicator vector, with 1 in the same position as the desired element in $\boldsymbol{\theta}$:

$$b_k = v; \qquad A_k = [0, \ldots, 1, \ldots, 0] \tag{A.12}$$

---

[3] Indicator notation, also known as "one-hot notation" is used to select one element from another vector, based on its position. An indicator vector is 1 in the same location as the element of interest, and 0 everywhere else.

For example, for $G = 3$, if it is known that 20% of individuals enter directly into risk group 2 upon entry into the model ($\hat{e}_2 = 0.20$), then $\boldsymbol{b}$ and A can be augmented with:

$$b_k = \left[\begin{array}{c} 0.20 \end{array} \right]; \qquad A_k = \left[\begin{array}{ccccccccc} \cdot & 1 & \cdot & \cdot & \cdot & \cdot & \cdot & \cdot & \cdot \end{array} \right] \qquad (A.13)$$

since $\hat{e}_2$ is the second element in $\boldsymbol{\theta}$. If the data suggest zero turnover from group i to group j, then Eq. (A.13) can also be used to set $\phi_{ij} = 0$.

The elements of $\hat{\boldsymbol{e}}$ must sum to one. Therefore, specifying all elements in $\hat{\boldsymbol{e}}$ will only provide $G - 1$ constraints, as the last element will be either redundant or violate the sum-to-one rule. As shown in Appendix B.3, the sum-to-one rule is actually implicit in Eq. (A.11), so it is not necessary to supply a constraint like $1 = \sum_i \hat{e}_i$.

3. Group duration. Type 1 constraints assume that the relative population size of each group remains constant. Another epidemiologic feature that epidemic models considered is whether or not the duration of time spent within a given risk group remains constant. For example, in STI transmission models that include formal sex work, it can be assumed that the duration in formal sex work work remains stable over time, such as in (Mishra et al., 2014; Boily et al., 2015). The duration δ_i is defined as the inverse of all rates of exit from the group:

$$\delta_i = \left(\mu + \sum_j \phi_{ij} \right)^{-1} \qquad (A.14)$$

Estimates of the duration in a given group can be sourced from cross-sectional survey data where participants are asked about how long they have engaged in a particular practice – such as sex in exchange for money (Watts et al., 2010). Data on duration may also be sourced from longitudinal data, where repeated measures of self-reported sexual behaviour, or proxy measures of sexual risk data, are collected (The DHS Program, 2019; ICAP, 2019). Data on duration in each risk group can then be used to define ϕ by rearranging Eq. (A.14) to yield: $\delta_i^{-1} - \mu = \sum_j \phi_{ij}$. For example, if for $G = 3$, the average duration in group 1 is known to be $\delta_1 = 5$ years, then $\boldsymbol{b}$ and A can be augmented with another row k:

$$b_k = \left[\begin{array}{c} 5^{-1} - \mu \end{array} \right]; \qquad A_k = \left[\begin{array}{ccccccccc} \cdot & \cdot & \cdot & 1 & 1 & \cdot & \cdot & \cdot & \cdot \end{array} \right] \qquad (A.15)$$

Similar to specifying all elements of $\hat{\boldsymbol{e}}$, specifying δ_i may result in conflicts or redundancies with other constraints. A conflict means it will not be possible to resolve values of ϕ which simultaneously satisfy all constraints, while a redundancy means that adding one constraint does not help resolve a unique set of values $\boldsymbol{\theta}$. For example, for $G = 3$, if Type 2 constraints are used to specify $\phi_{12} = 0.1$ and $\phi_{13} = 0.1$, and $\mu = 0.05$, then by Eq. (A.14), we must have $\delta_1 = 4$. Specifying any other value for δ_1 will result in a conflict, while specifying $\delta_1 = 4$ is redundant, since it is already implied. There are innumerable situations in which this may occur, so we do not attempt to describe them all. Section A.2.2 describes how to identify conflicts and redundancies when they are not obvious.

4. Turnover rate ratios. In many cases, it may be difficult to obtain estimates of a given turnover rate ϕ_{ij} for use in Type 2 constraints. However, it may be possible to estimate relative relationships between rates of turnover, such as:

$$r\,\phi_{ij} = \phi_{i'j'} \tag{A.16}$$

where r is a ratio relating the values of ϕ_{ij} and $\phi_{i'j'}$. For example, for $G = 3$, let T_1 be the total number of individuals entering group 1 due to turnover. If we know that 70% of T_1 originates from group 2, while 30% of T_1 originates from group 3, then $0.7\,T_1 = \phi_{23}\,x_2$ and $0.3\,T_1 = \phi_{13}\,x_1$, and thus: $\phi_{23}\left(\frac{0.3\,x_2}{0.7\,x_1}\right) = \phi_{13}$. This constraint can then be appended as another row k in $\boldsymbol{b}$ and A like:

$$b_k = \left[\begin{array}{c} 0 \end{array}\right]; \qquad A_k = \left[\begin{array}{cccccccc} \cdot & \cdot & \cdot & \cdot & \left(\frac{0.3\,x_2}{0.7\,x_1}\right) & \cdot & 1 & \cdot & \cdot \end{array}\right] \tag{A.17}$$

The example in Eq. (A.17) is based on what proportions of individuals entering a risk group j came from which former risk group i, but similar constraints may be defined based on what proportions of individuals exiting a risk group i enter into which new risk group j. It can also be assumed that the absolute number of individuals moving between two risk groups is equal, in which case the relationship is: $\phi_{ij}\left(\frac{x_i}{x_j}\right) = \phi_{ji}$. All constraints of this type will have $b_k = 0$.

Solving the System. Table A.1 summarizes the four types of constraints described above. Given a set of sufficient constraints on $\boldsymbol{\theta}$ to ensure exactly one solution, the system of equations Eq. (A.8) can be solved using $\boldsymbol{\theta} = A^{-1}\boldsymbol{b}$. The resulting values of $\hat{\boldsymbol{e}}$ and ϕ can then be used in the epidemic model.

However, we may find that we have an insufficient number of constraints, implying that there are multiple values of the vector $\boldsymbol{\theta}$ which satisfy the constraints. An insufficient number of constraints may be identified by a "rank deficiency" warning in numerical solvers of Eq. (A.8) (LAPACK, 1992). Even if A has G^2 rows, the system may have an insufficient number of constraints because some constraints are redundant. In this situation, we can pose the problem as a minimization problem, namely:

$$\boldsymbol{\theta}^* = \arg\min f(\boldsymbol{\theta}), \quad \text{subject to: } \boldsymbol{b} = A\,\boldsymbol{\theta}; \ \boldsymbol{\theta} \geq 0 \tag{A.18}$$

where f is a function which penalizes certain values of $\boldsymbol{\theta}$. For example, $f = ||\cdot||_2$ penalizes large values in $\boldsymbol{\theta}$, so that the smallest values of $\hat{\boldsymbol{e}}$ and ϕ which satisfy the constraints will be resolved.[4]

Similarly, we may find that no solution exists for the given constraints, since two or more constraints are in conflict. Conflicting constraints may be identified by a non-zero error in the solution to Eq. (A.8) (LAPACK, 1992). In this case, the conflict should be resolved by changing or removing one of the conflicting constraints.

---

[4] Numerical solutions to such problems are widely available, such as the Non-Negative Lease Squares solver (Lawson and Hanson, 1995), available in Python: https://docs.scipy.org/doc/scipy/reference/generated/scipy.optimize.nnls.html.

Name	Eq.	E.g.	Data requirements
1. Constant group size	(A.10)	(A.11)	all values of $\hat{x}_i$ and ν
2. Specified elements	(A.12)	(A.13)	any value of $\hat{e}_i$ or ϕ_{ij}
3. Group duration	(A.14)	(A.15)	any value of δ_i
4. Turnover rate ratios	(A.16)	(A.17)	any relationship between two turnover rates ϕ_{ij} and $\phi_{i'j'}$

ν: rate of population entry; ϕ_{ij}: rate of turnover from group i to group j; $\hat{x}_i$: proportion of individuals in risk group i;
$\hat{e}_i$: proportion of individuals entering into risk group i; δ_i: average duration spent in risk group i.

A.3. Previous Approaches

Few epidemic models of sexually transmitted infections with heterogeneity in risk have simulated turnover among risk groups, and those models which have simulated turnover have done so in various ways. In this section, we review three prior implementations of turnover and their assumptions. We then highlight how the approach proposed in Section A.2 could be used to achieve the same objectives.

Stigum et al. (1994) simulated turnover among $G = 2$ risk groups in a population with no exogenous entry or exit ($\nu = \mu = 0$ and hence $\hat{e}$ is not applicable). Turnover between the groups was balanced in order to maintain constant risk group sizes (Type 1 constraint),[5] while the rate of turnover from high to low was specified as κ (Type 2 constraint). Thus, the turnover system used by Stigum et al. (1994) can be written in the proposed framework as:

$$\begin{bmatrix} 0 \\ \kappa \end{bmatrix} = \begin{bmatrix} \hat{x}_1 & -\hat{x}_2 \\ 1 & \cdot \end{bmatrix} \begin{bmatrix} \phi_{12} \\ \phi_{21} \end{bmatrix}, \qquad \hat{e}_1 = \hat{e}_2 = 0 \tag{A.19}$$

Henry and Koopman (2015) also simulated turnover among $G = 2$ risk groups, but considered exogenous entry and exit, both at a rate μ. The authors used the notation f_i for our $\hat{x}_i$, and assumed that the population of individuals entering into the modelled population had the same distribution of risk groups as the modelled population itself: $\hat{e}_i = f_i$ (Type 2 constraint). The authors further maintained constant risk group sizes (Type 1 constraint) by analytically balancing turnover between the two groups using: $\phi_{12} = \omega \hat{x}_2$; $\phi_{21} = \omega \hat{x}_1$, where ω is a constant. However, it can be shown that this analytical approach is also the solution to the following combination of Type 1 and Type 2 constraints:

$$\begin{bmatrix} 0 \\ \omega f_2 \end{bmatrix} = \begin{bmatrix} f_1 & -f_2 \\ 1 & \cdot \end{bmatrix} \begin{bmatrix} \phi_{12} \\ \phi_{21} \end{bmatrix}, \qquad \hat{e}_i = f_i \tag{A.20}$$

---

[5] Due to its simplicity, this constraint is actually an example of both Type 1 and Type 4 constraints.

Eaton and Hallett (2014) simulated turnover among $G = 3$ risk groups, considering a distribution of risk among individuals entering into the modelled population $\hat{\boldsymbol{e}}$ which was different from $\hat{\boldsymbol{x}}$. Turnover was considered from high-to-medium, high-to-low, and medium-to-low risk, all with an equal rate ψ; the reverse transition rates were set to zero (six total Type 2 constraints). Given the unidirectional turnover, risk group sizes were maintained using the values of $\hat{e}_i$, computed using Type 1 constraints as follows:

$$
\begin{bmatrix} \nu x_1 + 2x_1\psi \\ \nu x_2 - x_1\psi + x_2\psi \\ \nu x_3 - x_1\psi - x_2\psi \end{bmatrix} = \begin{bmatrix} \nu & \cdot & \cdot \\ \cdot & \nu & \cdot \\ \cdot & \cdot & \nu \end{bmatrix} \begin{bmatrix} e_1 \\ e_2 \\ e_3 \end{bmatrix}, \qquad \begin{array}{l} \phi_{12} = \phi_{13} = \phi_{23} = \psi \\ \phi_{21} = \phi_{31} = \phi_{32} = 0 \end{array} \tag{A.21}
$$

In sum, the framework for modelling turnover presented in this section aims to generalize all previous implementations. In so doing, we hope to clarify the requisite assumptions, dependencies on epidemiologic data, and relationships between previous approaches.

B. Supplemental Equations

Table B.1: Notation

Symbol	Definition
i	risk group index
j	risk group index for "other" group in turnover
k	risk group index for "other" group in incidence
t	time
$\mathcal{S}_i$	number of susceptible individuals in risk group i
$\mathcal{I}_i$	number of infectious individuals in risk group i
$\mathcal{T}_i$	number of treated individuals in risk group i
N	total population size
ν	rate of population entry
μ	rate of population exit
ϕ_{ij}	rate of turnover from group i to group j
λ_i	force of infection among susceptibles in risk group i
τ	rate of treatment initiation among infected
$\hat{x}_i$	proportion of individuals in risk group i
$\hat{e}_i$	proportion of individuals entering into risk group i
δ_i	average duration spent in risk group i
C_i	number of partners per year among individuals in risk group i
β	probability of transmission per partnership
ρ_{ik}	probability of partnership formation between risk groups i and k

B.1. Model Equations

$$\frac{d}{dt}\mathcal{S}_i(t) = +\sum_j \phi_{ji}\mathcal{S}_j(t) - \sum_j \phi_{ij}\mathcal{S}_i(t) - \mu\mathcal{S}_i(t) + \nu\hat{e}_i N(t) - \lambda_i(t)\mathcal{S}_i(t) \tag{B.1a}$$

$$\frac{d}{dt}\mathcal{I}_i(t) = +\sum_j \phi_{ji}\mathcal{I}_j(t) - \sum_j \phi_{ij}\mathcal{I}_i(t) - \mu\mathcal{I}_i(t) \qquad\qquad + \lambda_i(t)\mathcal{S}_i(t) - \tau\mathcal{I}_i(t) \tag{B.1b}$$

$$\frac{d}{dt}\mathcal{T}_i(t) = +\underbrace{\sum_j \phi_{ji}\mathcal{T}_j(t)}_{\text{turnover into}} - \underbrace{\sum_j \phi_{ij}\mathcal{T}_i(t)}_{\text{turnover from}} - \underbrace{\mu\mathcal{T}_i(t)}_{\text{death}} \qquad\quad \underbrace{}_{\text{birth}} \qquad \underbrace{}_{\text{incidence}} + \underbrace{\tau\mathcal{I}_i(t)}_{\text{treatment}} \tag{B.1c}$$

30

B.2. Complete Example Turnover System

$$
\begin{array}{c}
\text{constant group size} \left\{ \begin{array}{c} \\ \\ \\ \end{array} \right. \\
\text{specified } e \left\{ \begin{array}{c} \\ \\ \\ \end{array} \right. \\
\text{group duration} \left\{ \begin{array}{c} \\ \\ \\ \end{array} \right. \\
\text{turnover rate ratios} \left\{ \begin{array}{c} \\ \\ \\ \end{array} \right.
\end{array}
\begin{bmatrix}
\nu x_1 \\ \nu x_2 \\ \nu x_3 \\ e_1^* \\ e_2^* \\ e_3^* \\ \delta_1^{-1} - \mu \\ \delta_2^{-1} - \mu \\ \delta_3^{-1} - \mu \\ 0 \\ 0 \\ 0
\end{bmatrix}
=
\begin{bmatrix}
\nu & \cdot & \cdot & -x_1 & -x_1 & x_2 & \cdot & x_3 & \cdot \\
\cdot & \nu & \cdot & x_1 & \cdot & -x_2 & -x_2 & \cdot & x_3 \\
\cdot & \cdot & \nu & \cdot & x_1 & \cdot & x_2 & -x_3 & -x_3 \\
1 & \cdot & \cdot & \cdot & \cdot & \cdot & \cdot & \cdot & \cdot \\
\cdot & 1 & \cdot & \cdot & \cdot & \cdot & \cdot & \cdot & \cdot \\
\cdot & \cdot & 1 & \cdot & \cdot & \cdot & \cdot & \cdot & \cdot \\
\cdot & \cdot & \cdot & 1 & 1 & \cdot & \cdot & \cdot & \cdot \\
\cdot & \cdot & \cdot & \cdot & \cdot & 1 & 1 & \cdot & \cdot \\
\cdot & \cdot & \cdot & \cdot & \cdot & \cdot & \cdot & 1 & 1 \\
\cdot & \cdot & \cdot & x_1 & \cdot & -x_2 & \cdot & \cdot & \cdot \\
\cdot & \cdot & \cdot & \cdot & x_1 & \cdot & \cdot & -x_3 & \cdot \\
\cdot & \cdot & \cdot & \cdot & \cdot & \cdot & x_2 & \cdot & -x_3
\end{bmatrix}
\begin{bmatrix}
e_1 \\ e_2 \\ e_3 \\ \phi_{12} \\ \phi_{13} \\ \phi_{21} \\ \phi_{23} \\ \phi_{31} \\ \phi_{32}
\end{bmatrix}
\tag{B.2}
$$

B.3. Redundancy in specifying all elements of $\hat{e}$

Whenever it is assumed that risk groups do not change size, G rows of the form shown in Eq. (A.11) are added to $\boldsymbol{b}$ and A:

$$
\boldsymbol{b} = \begin{bmatrix} \nu x_1 \\ \nu x_2 \\ \nu x_3 \end{bmatrix}; \qquad
A = \begin{bmatrix}
\nu & \cdot & \cdot & -x_1 & -x_1 & x_2 & \cdot & x_3 & \cdot \\
\cdot & \nu & \cdot & x_1 & \cdot & -x_2 & -x_2 & \cdot & x_3 \\
\cdot & \cdot & \nu & \cdot & x_1 & \cdot & x_2 & -x_3 & -x_3
\end{bmatrix}
\tag{A.11}
$$

After multiplying by $\boldsymbol{\theta}$, these G rows can be row-reduced by summing to obtain:

$$
\begin{aligned}
[\nu x_1 + \nu x_2 + \nu x_3] &= [\nu e_1 + \nu e_2 + \nu e_3 + 0\,\phi_{12} + 0\,\phi_{13} + 0\,\phi_{21} + 0\,\phi_{23} + 0\,\phi_{31} + 0\,\phi_{32}] \\
\nu\,[x_1 + x_2 + x_3] &= \nu\,[e_1 + e_2 + e_3]
\end{aligned}
\tag{B.3}
$$

which therefore implies that $\sum_i x_i = \sum_i e_i$, or equivalently $\sum_i \hat{x}_i = \sum_i \hat{e}_i = 1$. Thus, it is redundant to specify all G elements of $\hat{e}$, as the final element will be dictated by constant group size constraints.

B.4. Factors of Incidence

Substituting the proportional mixing definition of ρ_{ik} into the incidence equation, Eq. (3), we have:

$$
\begin{aligned}
\lambda_i &= C_i \sum_k \rho_{ik} \beta \frac{\mathcal{I}_k}{\mathcal{X}_k} \\
&= C_i \beta \sum_k \frac{C_k \mathcal{X}_k}{\sum_k C_k \mathcal{X}_k} \frac{\mathcal{I}_k}{\mathcal{X}_k} \\
&= C_i \beta \underbrace{\frac{\sum_k C_k \mathcal{I}_k}{\sum_k C_k \mathcal{X}_k}}_{f}
\end{aligned}
\tag{B.4}
$$

We can factor the term f as:

$$f = \frac{\sum_k C_k \mathcal{I}_k}{\sum_k C_k \mathcal{X}_k}$$
$$= \frac{\sum_k C_k \mathcal{I}_k}{\sum_k \mathcal{I}_k} \cdot \frac{\sum_k \mathcal{I}_k}{\sum_k \mathcal{X}_k} \cdot \frac{\sum_k \mathcal{X}_k}{\sum_k C_k \mathcal{X}_k} \tag{B.5}$$

which we recognize as the following terms:

$$= \hat{C}_\mathcal{I} \cdot \hat{\mathcal{I}} \cdot \hat{C}^{-1} \tag{B.6}$$

Namely,

1. $\hat{C}_\mathcal{I}$ is the average number of partners among infectious individuals

2. $\hat{\mathcal{I}}$ is the proportion of the population who are infectious (overall prevalence)

3. $\hat{C}$ is the average number of partners among all individuals (constant)

Therefore, only two non-constant factors control incidence per susceptible: 1) the average number of partners among infectious individuals $\hat{C}_\mathcal{I}$, and 2) overall prevalence $\hat{\mathcal{I}}$. The product of these factors $\hat{C}_\mathcal{I} \hat{\mathcal{I}}$, scaled by $\beta C_i / \hat{C}$, then gives λ_i. In fact, the incidence in each group individually is proportional to incidence overall, as C_i is only factor depending on i.

C. Supplemental Results

C.1. Equilibrium health states and rates of transition

(a) High risk

(b) Medium risk

(c) Low risk

(d) Overall
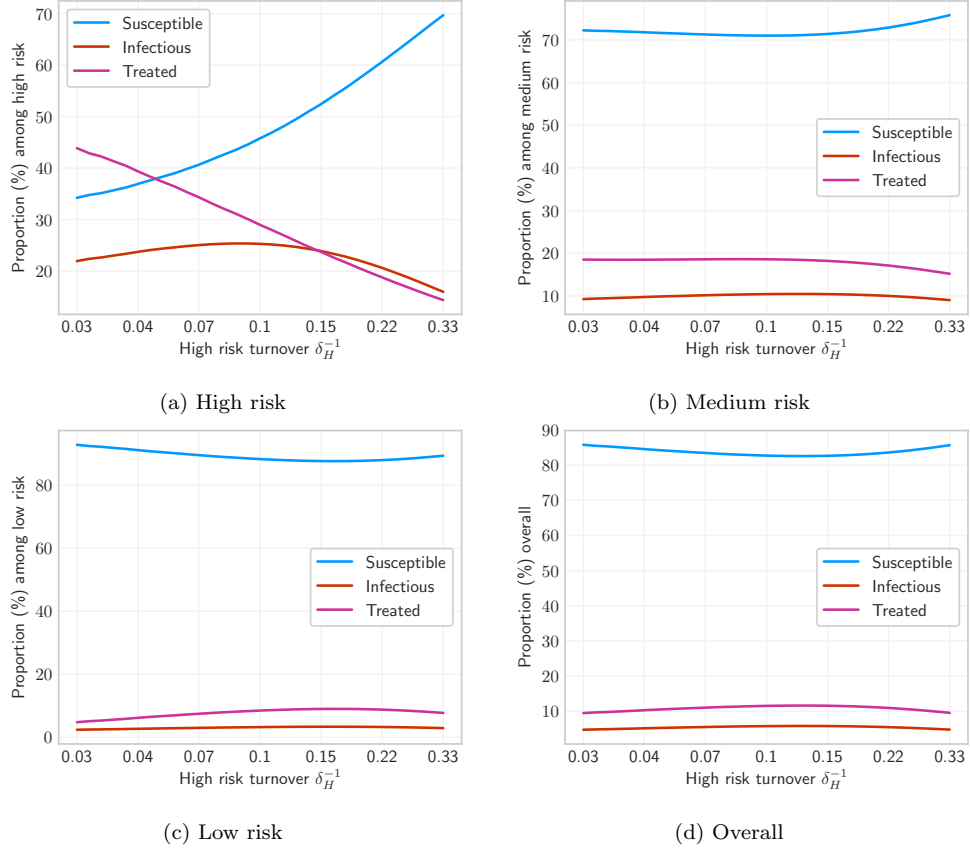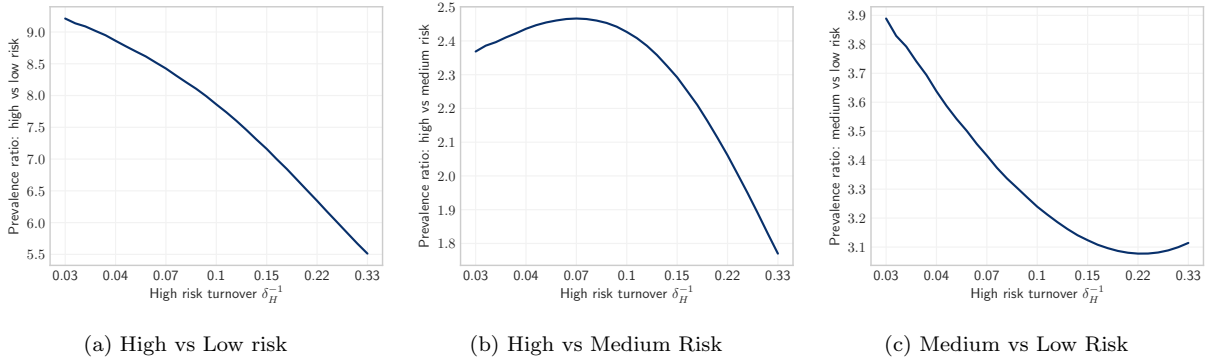
Figure C.1: Equilibrium health state proportions under different rates of turnover.

Turnover rate (log scale) is a function of the duration of time spent in the high risk group δ_H, where shorter time spent in the high risk group yields faster turnover. No turnover is indicated by $\delta_H^{-1} = 0.03$, due to population exit rate $\mu = 0.03$.
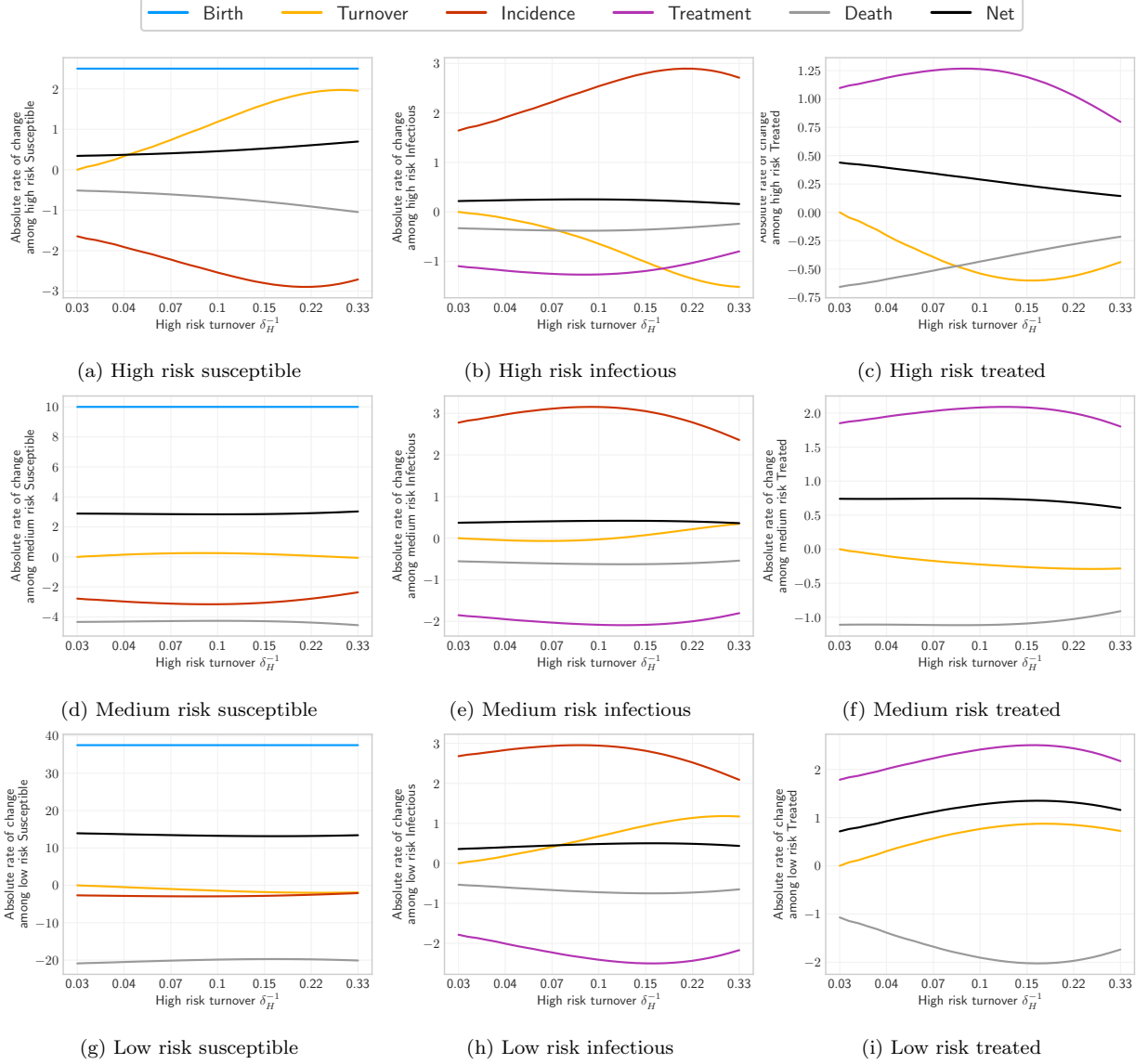
Figure C.2: Absolute rates of change at equilibrium (number of individuals gained/lost per year) among individuals in each health state and risk group, broken down by type of change: gain via births, loss/gain via incident infections, loss/gain via treatment, loss/gain via turnover, loss via death, and net change. Based on Eq. (B.1).

Turnover rate (log scale) is a function of the duration of time spent in the high risk group δ_H, where shorter time spent in the high risk group yields faster turnover. No turnover is indicated by $\delta_H^{-1} = 0.03$, due to population exit rate $\mu = 0.03$. Rates of change do not sum to zero due to population growth.
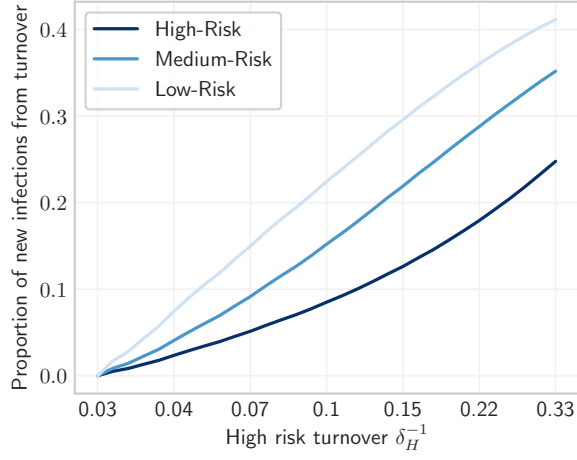
Figure C.3: Proportion of new infectious individuals in each risk group which are from turnover of infectious individuals, as opposed to incident infection of susceptible individuals in the risk group.

C.2. Equilibrium Prevalence Ratios

(a) High vs Low risk

(b) High vs Medium Risk

(c) Medium vs Low Risk

Figure C.4: Equilibrium prevalence ratios between risk groups under different rates of turnover.

Turnover rate (log scale) is a function of the duration of time spent in the high risk group δ_H, where shorter time spent in the high risk group yields faster turnover. No turnover is indicated by $\delta_H^{-1} = 0.03$, due to population exit rate $\mu = 0.03$.

C.3. Equilibrium Incidence

(a) High risk   (b) Medium risk   (c) Low risk
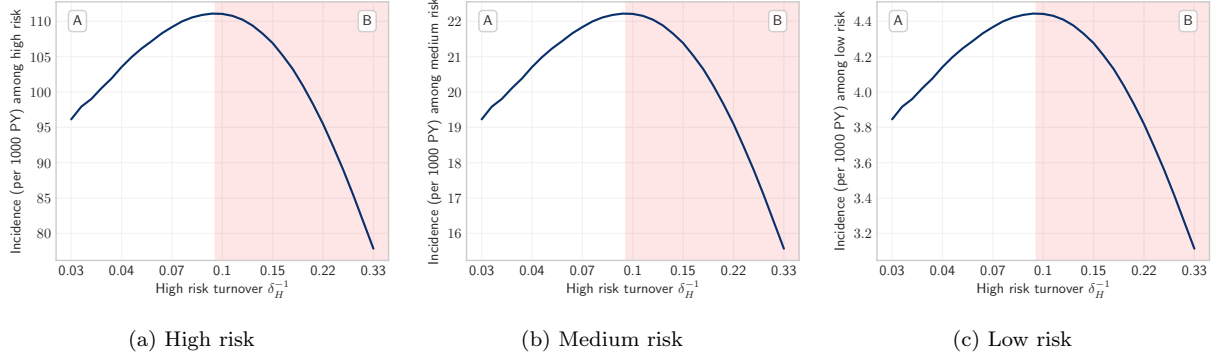
Figure C.5: Equilibrium incidence among high, medium, and low risk groups under different rates of turnover. Turnover rate (log scale) is a function of the duration of time spent in the high risk group δ_H, where shorter time spent in the high risk group yields faster turnover. No turnover is indicated by $\delta_H^{-1} = 0.03$, due to population exit rate $\mu = 0.03$. Incidence in each risk group is proportional to overall incidence with C_i as a scale factor.

(a) High vs low risk   (b) High vs medium risk   (c) Medium vs low risk
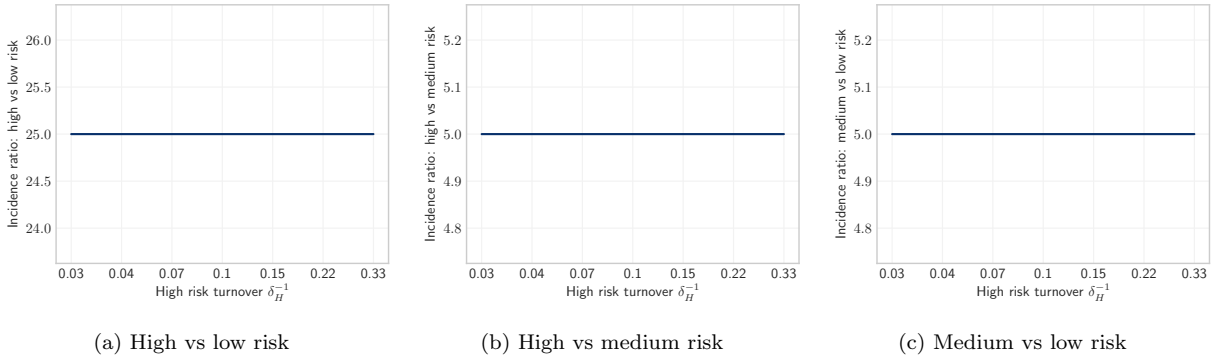
Figure C.6: Equilibrium incidence ratios between risk groups under different rates of turnover. Incidence ratios do not depend on turnover.

Turnover rate (log scale) is a function of the duration of time spent in the high risk group δ_H, where shorter time spent in the high risk group yields faster turnover. No turnover is indicated by $\delta_H^{-1} = 0.03$, due to population exit rate $\mu = 0.03$.

C.4. Equilibrium prevalence and number of partners before and after model fitting

(a) High risk

(b) Medium risk
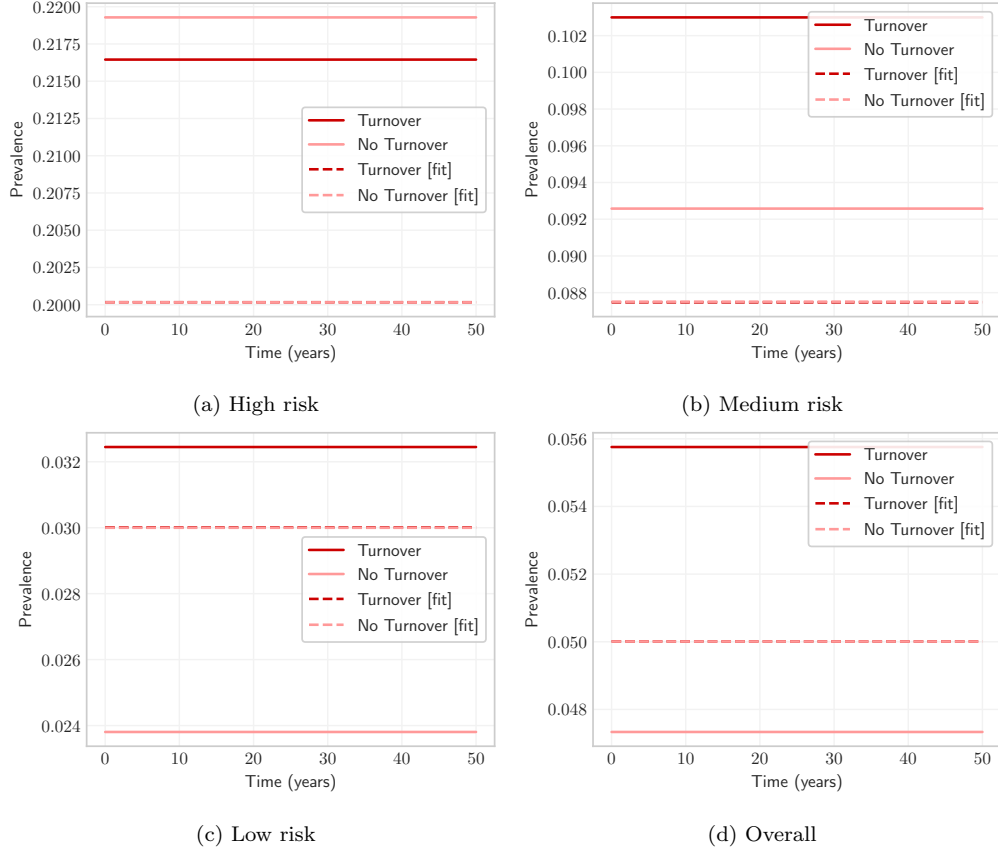
(c) Low risk

(d) Overall

Figure C.7: Equilibrium STI prevalence among high, medium, and low risk groups as well as overall, with and without turnover, and with and without fitted C_i to group-specific prevalence.
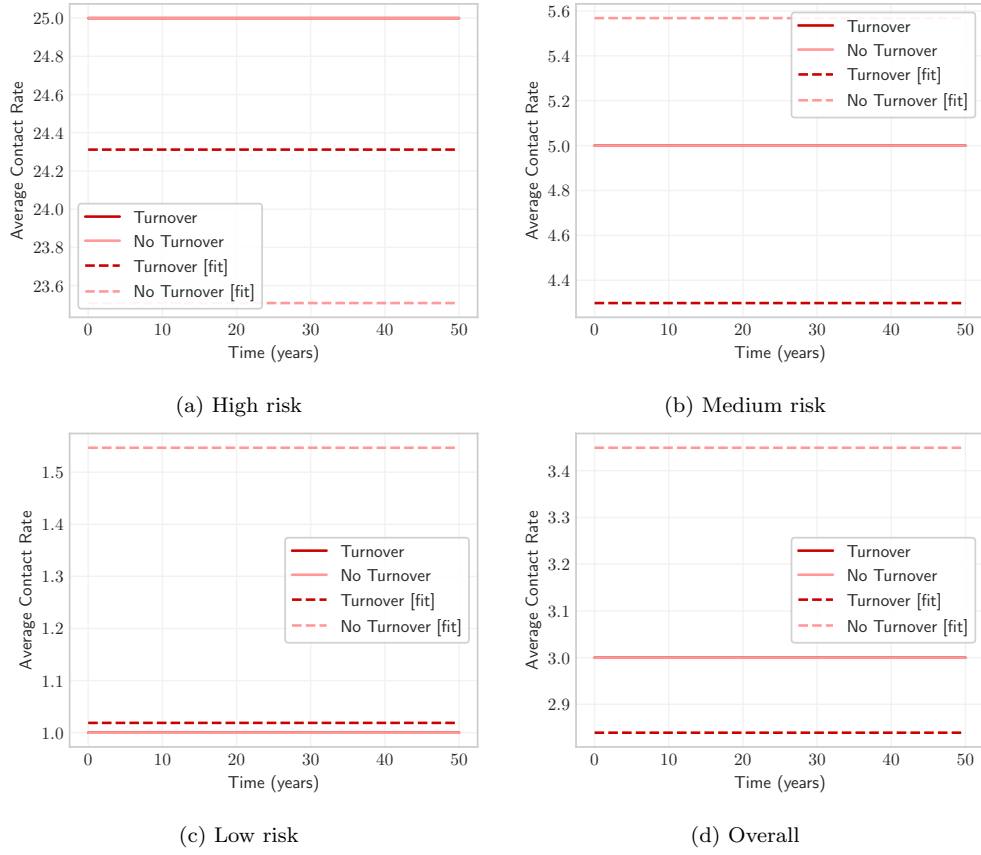
Figure C.8: Numbers of partners C_i among high, medium, and low risk groups as well as overall, with and without turnover, and with and without model fitting to group-specific prevalence.

C.5. Influence of turnover on the tPAF of the highest risk group before model fitting
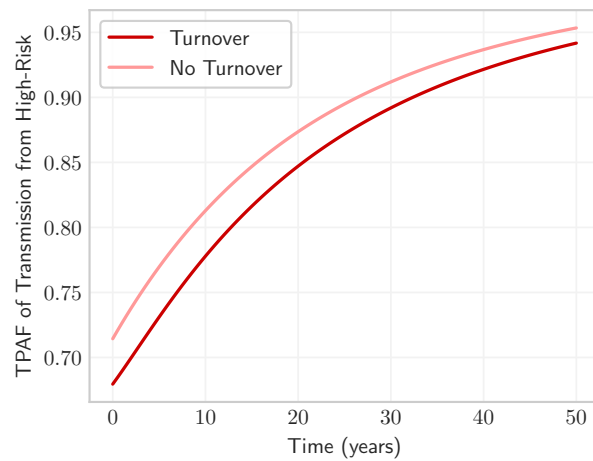
Figure C.9: Transmission population attributable fraction (tPAF) of the high risk group in models with and without turnover, before model fitting.

C.6. Effect of treatment rate on the influence of turnover on equilibrium prevalence

In order to examine the effect of treatment rate τ on the results of Experiment 1 – the influence of turnover on equilibrium prevalence – we recreated Figures 4 and 7 for a range of treatment rates $\tau \in [0.05, 1.0]$. The results are shown in Figure C.10.
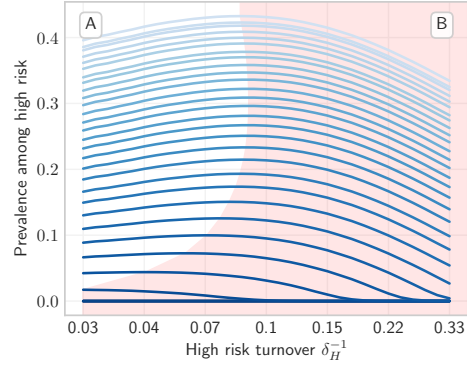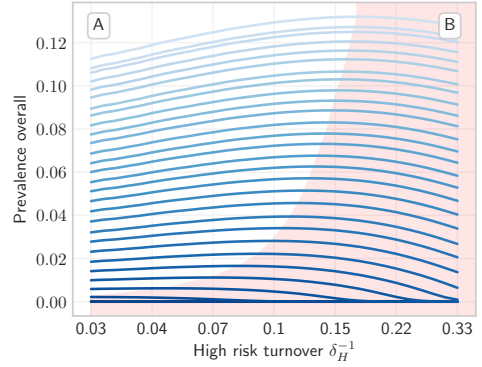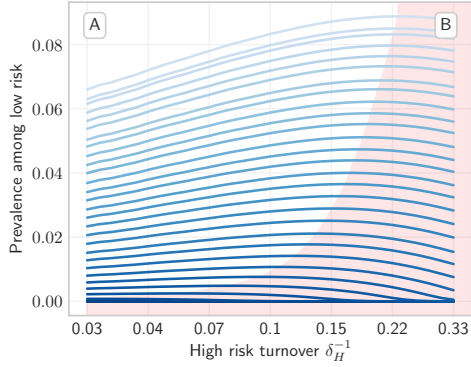
(a) Prevalence among high risk
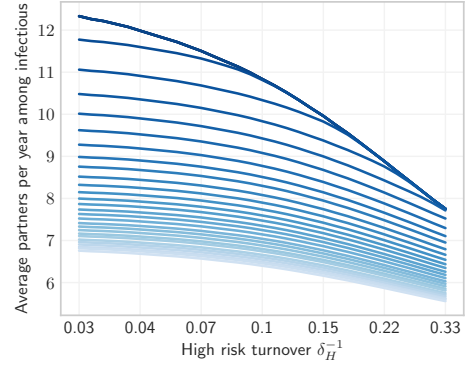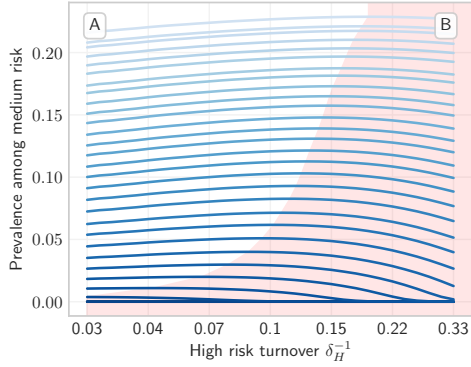
(b) Prevalence among medium risk

(c) Prevalence among low risk

(d) Average C among infectious individuals $\hat{C}_{\mathcal{I}}$

(e) Prevalence overall
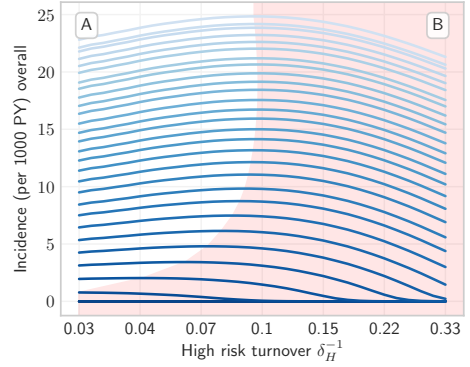
(f) Incidence overall λ

Figure C.10: Relationship between turnover rate and equilibrium STI prevalence in high, medium, and low risk groups, as well as overall STI prevalence and incidence, and average C among infectious individuals, for a range of treatment rates τ. Darker blue indicates higher treatment rate. The threshold turnover rate separating regions A and B decreases with treatment rate, meaning that increasing turnover becomes more likely to decrease equilibrium prevalence as treatment rate increases.

Turnover rate (log scale) is a function of the duration of time spent in the high risk group δ_H, where shorter time spent in the high risk group yields faster turnover. No turnover is indicated by $\delta_H^{-1} = 0.03$, due to population exit rate $\mu = 0.03$.